

AN ALGEBRAICALLY CONVERGING STOCHASTIC GRADIENT DESCENT ALGORITHM FOR GLOBAL OPTIMIZATION

BJÖRN ENGQUIST*, KUI REN†, AND YUNAN YANG‡

Abstract. We propose a new gradient descent algorithm with added stochastic terms for finding the global optimizers of nonconvex optimization problems, referred to as “AdaVar” here. A key component in the algorithm is the adaptive tuning of the randomness based on the value of the objective function. In the language of simulated annealing, the temperature is state-dependent. With this, we prove the global convergence of the algorithm with an algebraic rate both in probability and in the parameter space. This is an improvement over the classical rate from using a simpler control of the noise term. The convergence proof is based on the actual discrete setup of the algorithm. We also present several numerical examples to demonstrate the efficiency and robustness of the algorithm for reasonably complex objective functions.

Key words. stochastic gradient descent, global optimization, algebraic convergence

AMS subject classifications. 90C26, 90C15, 65K05

1. Introduction. For over a century and a half, the gradient descent method has been used for the optimization of real-valued functions. For minimization of function $f(x) \in C^1$ and $f : \mathbb{R}^d \mapsto \mathbb{R}$, the algorithm takes the form

$$(1.1) \quad X_{n+1} = X_n - \eta_n G(X_n),$$

where $G(x) = \nabla f(x)$, η_n is the step size, and $\{X_n\}$ are the iterates. Under proper conditions, the gradient descent algorithm converges to a local minimum within the basin of attraction. A sufficient convergence condition for strongly convex functions is $\eta_n = \eta < 2/L$, where L is the Lipschitz constant for $G(x)$. We will also satisfy this condition in the stochastic setting proposed below. When applied to general functions with many local minima, there is no guarantee of convergence to a global minimum through gradient descent (1.1).

For about half a century, an additional random term has been proposed for (1.1) in order to achieve global convergence for nonconvex functions. It results in a stochastic gradient descent algorithm

$$(1.2) \quad X_{n+1} = X_n - \eta_n G(X_n) + \sigma_n \psi_n,$$

where $\{\psi_n\}$ are random variables following a certain distribution, and we will assume $\psi_n \sim \mathcal{N}(0, I)$, the standard d -dimensional Gaussian, hereafter. The standard deviation σ_n controls the strength of the noise. Equation (1.2) represents the type of algorithm we focus on in this paper.

There are also many stochastic gradient descent techniques where the function and its gradient are intrinsically stochastic or where the gradient is stochastic from sampling, as is often the case in machine learning, e.g.,

$$(1.3) \quad X_{n+1} = X_n - \eta_n G(X_n; \xi_n),$$

where $G(x; \xi)$, parameterized by the random variable ξ , is a stochastic approximation to the true gradient $G(x)$. In this paper, we do not address algorithms on the common form (1.3) but will provide a numerical example in Section 5 where the adaptive variance is achieved by varying the batch size and offer a brief discussion on it in Section 6 under future directions. We also mention that the form (1.2) is sometimes used in the analysis of algorithm (1.3) with $G(X_n)$ as the expected value of $G(X_n, \xi_n)$.

In an algorithm of the form (1.2), which is the focus of this work, there is an obvious dilemma. The sequence $\{\sigma_n\}$ has to converge to zero as n increases even for convergence applied to convex functions.

*Department of Mathematics and the Oden Institute, The University of Texas, Austin, TX 78712; engquist@oden.utexas.edu

†Department of Applied Physics and Applied Mathematics, Columbia University, New York, NY 10027; kr2002@columbia.edu

‡Institute for Theoretical Studies, ETH Zürich, Zürich, Switzerland 8092; yunan.yang@eth-its.ethz.ch

On the other hand, if σ_n decreases too fast, the convergence will be to a local minimum and not the global one. This is analyzed in the classical papers [13, 5, 17, 15, 12] starting from the late 1980s, and the critical decay rate is $\mathcal{O}(\frac{1}{\sqrt{\log n}})$. The analyses were mainly based on the asymptotic limit as a stochastic differential equation related to the scaling,

$$(1.4) \quad X_{n+1} = X_n - \eta_n G(X_n) + \sqrt{2\eta_n T_n} \psi_n,$$

where $T_n \in \mathbb{R}^+$ is often referred to as the temperature parameter. To improve on this slow convergence rate, we propose an adaptive *state-dependent* σ_n ,

$$(1.5) \quad X_{n+1} = X_n - \eta_n G(X_n) + \sigma_n(f(X_n)) \psi_n.$$

This type of algorithm with an adaptive variance, which we label as “AdaVar” for future reference, can have a larger variance away from the minimum to explore the overall landscape and avoid trapping in a local minimum. It can then have a smaller variance for lower f -values, which is typically closer to the minimum. We will here use the simple form of the variance below based on the cutoff scalar value f_n with one variance for f -values above f_n and a smaller one for the case below the cutoff f_n . The sequence of scalar values $\{f_n\}$ are chosen by the user to implement the algorithm. That is,

$$(1.6) \quad \sigma_n(f(X_n)) = \begin{cases} \sigma_n^-, & f(X_n) \leq f_n, \\ \sigma_n^+, & f(X_n) > f_n. \end{cases}$$

See [Section 2](#) for details. Even this simple adaptive variance is powerful. We can improve on the slow logarithmic convergence rate and prove an algebraic rate, $\mathcal{O}(n^{-\alpha})$, $\alpha > 0$, in both space and probability. We also assume that f has a Lipschitz continuous gradient and a unique global minimum. Furthermore, there should be an open set containing the global minimum where f is strongly convex. The convergence theorem and the proofs are for the actual discrete algorithm and will be given in [Section 2](#) and [Section 3](#).

There are numerous similar strategies for global convergence, and many of them use multiple sequences of X_n values [24, Section 1]. In the simulated annealing algorithm [16], all new points that lower the objective function are accepted, and, with a certain probability, points that raise the objective function value are also accepted, which is the key to avoiding local-minima trapping. In parallel tempering and its variants, such as the replica exchange method [8], Metropolis type of acceptance-rejection strategies are used to alternate between different sequences of X_n . When the multimodality of the objective function is mild, methods known as “multistart” [24, Section 2.6] and “random initialization” [4] can be efficient to find the global minimum. In consensus-based optimization [3, 21], a group of particles explore the optimization landscape simultaneously under some stochastic influence and then build a consensus at the position of the weighted mean that is located near the global minimizer. In classical genetic algorithms (see the nice book [22] for several examples), global convergence is achieved by random seeding such that one of the locally converging sequences will converge to the global minimum. Optimal control problems aiming at selecting optimal tempering schemes to reduce computational cost have also been studied [11]. The algorithm proposed here can, of course, also be used in parallel but is powerful even as a single sequence method, as is seen in [Subsection 5.1.2](#). The basin of attraction for the global minimum has a volume proportionally 10^{-7} of the volume of the entire domain, but the implicit seeding from the AdaVar algorithm practically converges in $\mathcal{O}(10^4)$ iterations, which is much faster than what random seeding could give.

The rest of the paper is organized as follows. The mathematical setup and main result of the paper are presented in [Section 2](#). We then prove the main theorem in [Section 3](#) through several lemmas. In [Section 4](#), we discuss algorithmic details in terms of the implementation of the proposed algorithm and several key parameter estimations. In [Section 5](#), we present numerical examples illustrating the effectiveness of adaptive state-dependent variance. This includes a couple of examples based on settings that are not studied in this paper but will be the focus of forthcoming research. One example deals with the type of optimization common in machine learning, and the other with gradient-free optimization. These extensions are further discussed in the future directions as part of [Section 6](#).

2. Statement of Main Result. While the decay $\mathcal{O}(\frac{1}{\sqrt{\log n}})$ in σ_n in (1.2) ensures the convergence of the iterates X_n to the global minimizer x^* in probability [15], it only gives a logarithmic convergence rate. In this paper, we propose a new SGD algorithm with an *algebraic* rate of convergence. The faster convergence here is achieved by having an adaptive and state-dependent noise term in the form of (1.5).

Let us consider a nonconvex objective function $f : \mathbb{R}^d \mapsto \mathbb{R}$, $f \in C^1$ and $G(x) = \nabla f(x)$. We have the following additional assumptions for the function $f(x)$.

A1 On a bounded open set $\Omega_{sc} \subset \mathbb{R}^d$, $f \in C^2(\Omega_{sc})$ is strongly convex, and $b_1 I \preceq \nabla^2 f(x) \preceq b_2 I$, where $0 < b_1 \leq b_2 < \infty$, $x \in \Omega_{sc}$, and $I \in \mathbb{R}^{d \times d}$ is the identity matrix;

A2 $f(x)$ has a unique global minimizer x^* that lies strictly inside Ω_{sc} and $f(x^*) = f^*$.

We follow the two-stage adaptive variance (1.6) and consider the following discrete algorithm for minimizing f . Let $\mathfrak{X} \subset \mathbb{R}^d$ be a non-empty compact set such that $\Omega_{sc} \subseteq \mathfrak{X}$. Given any $X_0 \in \mathfrak{X}$, we propose an iterative optimization process for $n \geq 1$,

$$(2.1) \quad X_{n+1} = \begin{cases} X_n - \eta_n G(X_n) + \sigma_n \psi_n, & X_n \in \Omega_n, \\ \phi_n, & X_n \in \Omega_n^c = \mathbb{R}^d \setminus \Omega_n, \end{cases}$$

where $\sigma_n \in \mathbb{R}^+$ is the standard deviation of the Gaussian random term, and $\{\phi_n\}$ are i.i.d. random variables following $\mathcal{U}(\mathfrak{X})$, the uniform distribution on \mathfrak{X} . The subset $\Omega_n \subset \mathbb{R}^d$, $\forall n \in \mathbb{N}$, is the f_n -sublevel set of function $f(x)$ defined as

$$(2.2) \quad \Omega_n = \{x \in \mathbb{R}^d : f(x) \leq f_n\},$$

where the real sequence $\{f_n\}$ monotonically decreases as n increases. Note that the sublevel sets satisfy $\Omega_{n_1} \subseteq \Omega_{n_2}$ if $n_1 \geq n_2$. Without loss of generality, we assume that $\Omega_0 \subset \mathfrak{X}$ for the chosen starting iterate X_0 , and consequently, we have $\Omega_n \subset \mathfrak{X}$, $\forall n \in \mathbb{N}$. The set \mathfrak{X} can be considered as the target search domain as (2.1) enforces the iterates $\{X_n\}$ to always come back to \mathfrak{X} .

Let us emphasize that (2.1) is simply the limiting case of (1.5) together with the two-stage adaptive variance (1.6), when σ_n^+ is set to be $+\infty$.

We will use the following notations consistently throughout the paper. Given a measurable set $A \subset \mathbb{R}^d$ with a nonzero Lebesgue measure, i.e., $|A| > 0$,

$$(2.3) \quad \begin{aligned} X_n^+ &:= X_n - \eta_n G(X_n), \\ k_n(y, x) &:= \left(\sqrt{2\pi}\sigma_n\right)^{-d} \exp\left(-\frac{|y - x^+|^2}{2\sigma_n^2}\right), \quad x^+ = x - \eta_n G(x), \end{aligned}$$

$$(2.4) \quad p_n(A) := \mathbb{P}(X_{n+1} \in A | X_n \in \Omega_n) = \frac{\int_{\Omega_n} \left(\int_A k_n(y, x) dy\right) d\mu_n(x)}{\int_{\Omega_n} d\mu_n(x)},$$

$$(2.5) \quad q_n(A) := \mathbb{P}(X_{n+1} \in A | X_n \in \Omega_n^c) = \frac{|A \cap \mathfrak{X}|}{|\mathfrak{X}|},$$

where μ_n is the probability measure associated with the random variable X_n . Thus, p_n and q_n represent the conditional probability given $X_n \in \Omega_n$ and $X_n \in \Omega_n^c$, respectively.

The pinnacle of the proposed algorithm is how we control the decay rates of σ_n and $|\Omega_n|$ simultaneously such that

1. $\sigma_n \rightarrow 0$ as $n \rightarrow \infty$; That is, the noise variance upon the trusted region decreases.
2. $|\Omega_n| \rightarrow 0$ as $n \rightarrow \infty$, due to the monotonic decrease of f_n .

We add a few more assumptions that concretely determine the iteration in (2.1), based on which the main theorem holds. Let c_0 be the radius of a ball in \mathbb{R}^d with unit volume.

B1 The step size in (2.1) is a constant where $\eta_n = \eta < 2/b_2$.

B2 For $n \geq 1$, $\sigma_n = \frac{c_0 \sqrt[2]{|\Omega_n|}}{\sqrt{\log n}}$ where Ω_n depends on f_n based on (2.2).

B3 $|\Omega_{n+1}| = |\Omega_0|n^{-\alpha}$, $\forall n \geq 1$, where $0 < \alpha < \alpha^* = \frac{(c^*)^2}{2}$, $c^* = \frac{2\eta b_2 - \eta^2 b_2^2}{4} \left(\frac{b_1}{b_2}\right)^{\frac{3}{2}}$; $|\Omega_1| = |\Omega_0|$.

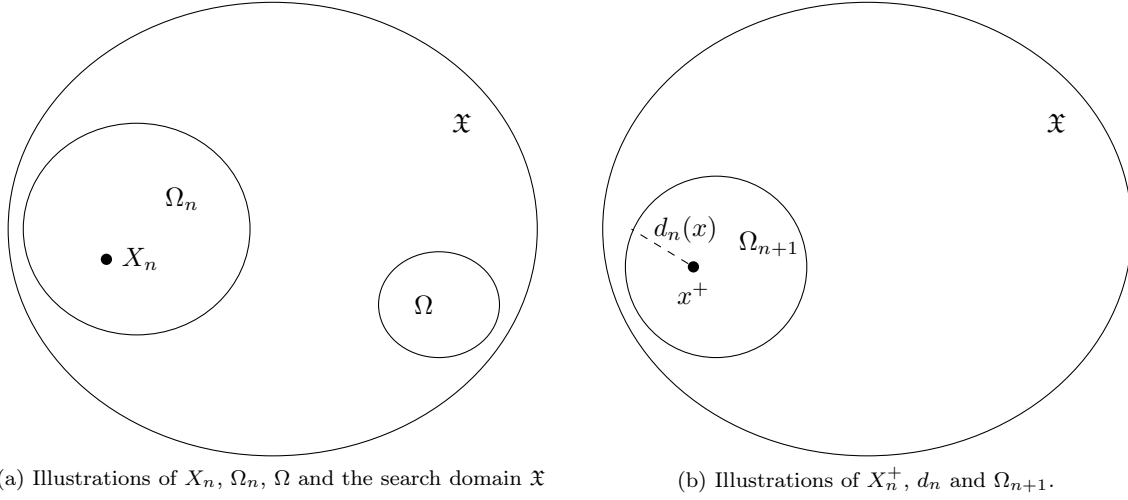


Fig. 1: Illustrations for proofs of Property One in Section 3.1 and Property Two in Section 3.2. The set Ω in (a) is used in all lemmas in Section 3.1. The distance $d_n(x)$ in (b) is defined in (3.26).

We remark that if $f_n \equiv f_0$ for all n , we have $\Omega_n \equiv \Omega_0$. Consequently, **B2** becomes the classical decay rate $\sigma_n = \mathcal{O}(\frac{1}{\sqrt{\log n}})$. Our proposed algorithm (2.1) also reduces to the classical case (1.4) for which the $\mathcal{O}(\frac{1}{\sqrt{\log n}})$ decay rate is optimal to guarantee global convergence [13, 17, 15, 14]. Besides, if $\eta = 1/b_2$, the upper bound α^* for α in **B3** is maximized.

We are ready to state the main theorem of this paper.

THEOREM 2.1. *Let **A1-A2** and **B1-B3** hold and the iterates $\{X_n\}$ follow the stochastic gradient descent algorithm (2.1). Then, $\exists N \in \mathbb{N}$ such that $\forall n \geq N$,*

$$\mathbb{P}\left(|X_n - x^*| > \mathfrak{c}_1 n^{-\alpha/d}\right) \leq \mathfrak{c}_2 n^{\alpha-\alpha_2},$$

where $\alpha_2 = \frac{\alpha}{2} + \frac{(c^*)^2}{4}$. Here, $\mathfrak{c}_1, \mathfrak{c}_2$ are constants that depend on b_1 and b_2 .

The main goal here is to prove that there is an algorithm of AdaVar type with algebraic convergence rates. The algorithm depends on the volume of Ω_n as a function of f_n and the parameters b_1 and b_2 . From the proof in Section 3 and the analysis in Section 4, it is clear that these estimates can be very rough, and we would still have algebraic convergence but potentially with a smaller α .

3. Convergence Proof. The proof of Theorem 2.1 is divided into three parts. In Subsection 3.1, we first present five lemmas demonstrating that the iterates following algorithm (2.1) will visit any subset of the domain of interest with a nonzero measure with high probability, under the assumptions in Section 2. In Subsection 3.2, we present another three lemmas to obtain the lower and upper bounds for the key conditional probability $p_n(\Omega_{n+1}^c)$. Finally, in Subsection 3.3, we combine all the previous lemmas and prove that the iterates converge to the global minimizer in probability with concrete algebraic convergence rates.

3.1. Property One: Full Coverage of the Entire Domain. Given the initial iterate X_0 , we are interested in finding the global minimum within the set \mathfrak{X} . For an arbitrary measurable set $\Omega \subseteq \mathfrak{X}$ where $|\Omega| \neq 0$, we use the following shorthand notations hereafter:

- the event $X_n \in \Omega_n$ as A_n ,
- the event $X_n \notin \Omega_n$ as A_n^c ,
- the event $X_n \in \Omega$ as B_n ,
- the event $X_n \notin \Omega$ as B_n^c .

See Figure 1a for illustrations of Ω , Ω_n and related sets. We define l_{n+1} using (2.4) and (2.5) where

$$(3.1) \quad l_{n+1} = \mathbb{P}(B_{n+1}|A_n^c) \min \left(\min_{x \in \Omega_{n-1}} \mathbb{P}(A_n^c|X_{n-1} = x), \mathbb{P}(A_n^c|A_{n-1}^c) \right).$$

It is clear that $\min_{x \in \Omega_{n-1}} \mathbb{P}(A_n^c|X_{n-1} = x)$ is a lower bound for $\mathbb{P}(A_n^c|A_{n-1}^c)$. To see that, we expand

$$(3.2) \quad \begin{aligned} \mathbb{P}(A_n^c|A_{n-1}^c) &= \mathbb{P}(X_n \notin \Omega_n | X_{n-1} \in \Omega_{n-1}) = \frac{\int_{\Omega_{n-1}} \left(\int_{\Omega_n^c} k_n(y, x) dy \right) d\mu_{n-1}(x)}{\int_{\Omega_{n-1}} d\mu_{n-1}(x)} \\ &\geq \min_{x \in \Omega_{n-1}} \int_{\Omega_n^c} k_n(y, x) dy = \min_{x \in \Omega_{n-1}} \mathbb{P}(A_n^c|X_{n-1} = x), \end{aligned}$$

where μ_n is the probability measure associated with the random variable X_n (which we do not need to know exactly). The following Lemma 3.1 and Lemma 3.2 show that l_{n+1} is a lower bound for both $\mathbb{P}(B_{n+1})$ and $\mathbb{P}(B_{n+1}|B_{n-1}^c)$.

LEMMA 3.1. *For any closed subset $\Omega \subseteq \mathfrak{X}$, $\mathbb{P}(B_{n+1}) := \mathbb{P}(X_{n+1} \in \Omega) \geq l_{n+1}$.*

Proof. By the law of total probability, we have

$$\begin{aligned} \mathbb{P}(B_{n+1}) &= \mathbb{P}(B_{n+1}|A_n \cap A_{n-1}) \mathbb{P}(A_n \cap A_{n-1}) + \mathbb{P}(B_{n+1}|A_n \cap A_{n-1}^c) \mathbb{P}(A_n \cap A_{n-1}^c) + \\ &\quad \mathbb{P}(B_{n+1}|A_n^c \cap A_{n-1}) \mathbb{P}(A_n^c \cap A_{n-1}) + \mathbb{P}(B_{n+1}|A_n^c \cap A_{n-1}^c) \mathbb{P}(A_n^c \cap A_{n-1}^c). \end{aligned}$$

We use the last two terms on the right-hand side to give a lower bound for $\mathbb{P}(B_{n+1})$.

$$\begin{aligned} \mathbb{P}(B_{n+1}) &\geq \min \left(\mathbb{P}(B_{n+1}|A_n^c \cap A_{n-1}), \mathbb{P}(B_{n+1}|A_n^c \cap A_{n-1}^c) \right) \left(\mathbb{P}(A_n^c \cap A_{n-1}) + \mathbb{P}(A_n^c \cap A_{n-1}^c) \right) \\ &= \mathbb{P}(B_{n+1}|A_n^c) \left(\mathbb{P}(A_n^c \cap A_{n-1}) + \mathbb{P}(A_n^c \cap A_{n-1}^c) \right) \\ &= \mathbb{P}(B_{n+1}|A_n^c) \left(\theta \mathbb{P}(A_n^c|A_{n-1}) + (1 - \theta) \mathbb{P}(A_n^c|A_{n-1}^c) \right) \quad (\theta = \mathbb{P}(A_{n-1})) \\ &\geq \mathbb{P}(B_{n+1}|A_n^c) \min \left(\mathbb{P}(A_n^c|A_{n-1}), \mathbb{P}(A_n^c|A_{n-1}^c) \right) \\ &\geq l_{n+1}. \end{aligned}$$

The first equality above is based on the Markov property of the algorithm in (2.1). The last inequality comes from (3.2). The proof is complete. \square

LEMMA 3.2. *For any closed subset $\Omega \subseteq \mathfrak{X}$ and $n \geq 1$, $\mathbb{P}(B_{n+1}|B_{n-1}^c) \geq l_{n+1}$.*

Proof. We define disjoint events $D_{n-1}^1 = A_{n-1} \cap B_{n-1}^c$ and $D_{n-1}^2 = A_{n-1}^c \cap B_{n-1}^c$. It is then clear that

$$(3.3) \quad \begin{aligned} \mathbb{P}(B_{n+1}|B_{n-1}^c) &= \mathbb{P}(B_{n+1}|D_{n-1}^1 \cup D_{n-1}^2) \\ &= \theta \mathbb{P}(B_{n+1}|D_{n-1}^1) + (1 - \theta) \mathbb{P}(B_{n+1}|D_{n-1}^2) \quad \left(\theta = \frac{\mathbb{P}(D_{n-1}^1)}{\mathbb{P}(B_{n-1}^c)} \right) \\ &\geq \min \left(\mathbb{P}(B_{n+1}|D_{n-1}^1), \mathbb{P}(B_{n+1}|D_{n-1}^2) \right). \end{aligned}$$

For $\mathbb{P}(B_{n+1}|D_{n-1}^1)$, we continue the arguments with conditional probability.

$$(3.4) \quad \begin{aligned} \mathbb{P}(B_{n+1}|D_{n-1}^1) &\geq \mathbb{P}(B_{n+1} \cap A_n^c|D_{n-1}^1) \\ &= \mathbb{P}(B_{n+1}|A_n^c \cap D_{n-1}^1) \mathbb{P}(A_n^c|D_{n-1}^1) = \mathbb{P}(B_{n+1}|A_n^c) \mathbb{P}(A_n^c|D_{n-1}^1), \end{aligned}$$

due to the Markov property of the algorithm. Similarly, one can show that

$$(3.5) \quad \mathbb{P}(B_{n+1}|D_{n-1}^2) \geq \mathbb{P}(B_{n+1}|A_n^c) \mathbb{P}(A_n^c|D_{n-1}^2).$$

Plugging both (3.4) and (3.5) into (3.3), we have

$$\mathbb{P}(B_{n+1}|B_{n-1}^c) \geq \mathbb{P}(B_{n+1}|A_n^c) \min \left(\mathbb{P}(A_n^c|D_{n-1}^1), \mathbb{P}(A_n^c|D_{n-1}^2) \right).$$

Note that

$$\begin{aligned} \mathbb{P}(A_n^c|D_{n-1}^1) &= \mathbb{P}(A_n^c|X_{n-1} \in \Omega_{n-1} \cap \Omega^c) \\ &= \frac{\int_{\Omega_{n-1} \cap \Omega^c} \left(\int_{\Omega_n^c} k_n(y, x) dy \right) d\mu_{n-1}(x)}{\int_{\Omega_{n-1} \cap \Omega^c} d\mu_{n-1}(x)} \\ &\geq \min_{x \in \Omega_{n-1} \cap \Omega^c} \int_{\Omega_n^c} k_n(y, x) dy \\ &\geq \min_{x \in \Omega_{n-1}} \int_{\Omega_n^c} k_n(y, x) dy = \min_{x \in \Omega_{n-1}} \mathbb{P}(A_n^c|X_{n-1} = x), \end{aligned}$$

where the last inequality holds since $\Omega_{n-1} \cap \Omega^c \subseteq \Omega_{n-1}$. Similarly, we have

$$\mathbb{P}(A_n^c|D_{n-1}^2) = \mathbb{P}(A_n^c|X_{n-1} \in \Omega_{n-1}^c \cap \Omega^c) = \frac{|\Omega_n^c|}{|\mathcal{X}|} = \mathbb{P}(A_n^c|X_{n-1} \in \Omega_{n-1}^c) = \mathbb{P}(A_n^c|A_{n-1}^c).$$

Therefore, by combining these two together, we have

$$\mathbb{P}(B_{n+1}|B_{n-1}^c) \geq \mathbb{P}(B_{n+1}|A_n^c) \min \left(\min_{x \in \Omega_{n-1}} \mathbb{P}(A_n^c|X_{n-1} = x), \mathbb{P}(A_n^c|A_{n-1}^c) \right) = l_{n+1}.$$

We then obtain l_{n+1} as the lower bound for $\mathbb{P}(B_{n+1}|B_{n-1}^c)$. \square

Next, we will provide lower bounds for $\mathbb{P}(B_{n+1}|A_n^c)$, $\mathbb{P}(A_n^c|A_{n-1}^c)$ and $\min_{x \in \Omega_{n-1}} \mathbb{P}(A_n^c|X_{n-1} = x)$ with the goal of estimating l_{n+1} . For the third term, we introduce the following lemma.

LEMMA 3.3. *Given any $x \in \mathbb{R}^d$ and $\sigma, V \in \mathbb{R}^+$, let $\mathcal{M}_V = \{A \subseteq \mathbb{R}^d : |A| = V\}$. For any set $A \in \mathcal{M}_V$, we have*

$$(3.6) \quad \left(\sqrt{2\pi}\sigma \right)^{-d} \int_A \exp \left(-\frac{|y-x|^2}{2\sigma^2} \right) dy \leq \left(\sqrt{2\pi}\sigma \right)^{-d} \int_{B(x;R)} \exp \left(-\frac{|y-x|^2}{2\sigma^2} \right) dy,$$

where $B(x;R) \in \mathcal{M}_V$ is a ball centered at x with radius $R = c_0 \sqrt[d]{V}$, $c_0 = \pi^{-\frac{1}{2}} \sqrt[d]{\Gamma\left(\frac{d}{2} + 1\right)}$ being the radius for a ball of unit volume in \mathbb{R}^d .

Proof. First, recall that the volume of a d -dimensional ball of radius R is $\frac{(\sqrt{\pi}R)^d}{\Gamma(\frac{d}{2}+1)}$, where $\Gamma(s)$ is the Gamma function. Thus, a d -dimensional ball of radius $R = c_0 \sqrt[d]{V}$ has volume V .

Next, we define a function $f(x, y; \sigma) = (\sqrt{2\pi}\sigma)^{-d} e^{-\frac{|y-x|^2}{2\sigma^2}}$. Given any $A \in \mathcal{M}_V$,

$$\begin{aligned} \int_A f(x, y; \sigma) dy &= \int_{A \cap B(x; R)} f(x, y; \sigma) dy + \int_{A \setminus B(x; R)} f(x, y; \sigma) dy \\ &\leq \int_{A \cap B(x; R)} f(x, y; \sigma) dy + |A \setminus B(x; R)| \max_{y \in A \setminus B(x; R)} f(x, y; \sigma) \\ (3.7) \quad &\leq \int_{A \cap B(x; R)} f(x, y; \sigma) dy + |A \setminus B(x; R)| e^{-\frac{R^2}{2\sigma^2}}, \end{aligned}$$

$$\begin{aligned} \int_{B(x; R)} f(x, y; \sigma) dy &= \int_{A \cap B(x; R)} f(x, y; \sigma) dy + \int_{B(x; R) \setminus A} f(x, y; \sigma) dy \\ &\geq \int_{A \cap B(x; R)} f(x, y; \sigma) dy + |B(x; R) \setminus A| \min_{y \in B(x; R) \setminus A} f(x, y; \sigma) \\ (3.8) \quad &\geq \int_{A \cap B(x; R)} f(x, y; \sigma) dy + |B(x; R) \setminus A| e^{-\frac{R^2}{2\sigma^2}}. \end{aligned}$$

Since $|B(x; R) \setminus A| = |A \setminus B(x; R)|$ as a result of $|B(x; R)| = |A| = V$, we conclude with (3.6) by combining (3.7) with (3.8). \square

Let us define a key ratio that will be used in the rest of the section,

$$s_n = c_0 \sqrt[d]{|\Omega_n|} / \sigma_n.$$

We can then derive a lower bound for l_{n+1} for large n in terms of s_n .

LEMMA 3.4. *Under the assumptions in **A1**, **A2**, **B2** and **B3**, for any $\Omega \subset \mathfrak{X}$ where $|\Omega| \neq 0$, $\exists M \in \mathbb{N}$ such that for all $n \geq M$, l_{n+1} defined in (3.1) has a lower bound*

$$(3.9) \quad l_{n+1} \geq c s_{n-1}^d e^{-s_{n-1}^2},$$

where the constant c only depends on $|\Omega|$ and d .

Proof. First, we aim to obtain a lower bound for $\min_{x \in \Omega_{n-1}} \mathbb{P}(A_n^c | X_{n-1} = x)$. Since $\Omega_{n-1}^c \subseteq \Omega_n^c$, we have $\mathbb{P}(X_n \in \Omega_n^c | X_{n-1} = x) \geq \mathbb{P}(X_n \in \Omega_{n-1}^c | X_{n-1} = x)$ for any fixed x . It is then sufficient to derive a lower bound for the right-hand side. Next, we focus on $\min_{x \in \Omega_n} \mathbb{P}(X_{n+1} \in \Omega_n^c | X_n = x)$ by shifting the index from $n-1$ to n .

Based on (2.4), for any fixed $x \in \Omega_n$,

$$\mathbb{P}(X_{n+1} \in \Omega_n^c | X_n = x) = \left(\sqrt{2\pi}\sigma_n \right)^{-d} \int_{\Omega_n^c} \exp \left(-\frac{|y-x|^2}{2\sigma_n^2} \right) dy,$$

where x^+ follows (2.3). Consider a ball $\mathcal{B}_n = B(x^+; R_n) \subset \mathbb{R}^d$ centered at x^+ with radius $R_n = c_0 \sqrt[d]{|\Omega_n|}$. Hence, $|\mathcal{B}_n| = |\Omega_n|$. We define another ball $\mathcal{B}'_n = B(x^+; \sqrt{2}R_n)$, also centered at x^+ but with a larger radius $\sqrt{2}R_n$. Consequently, $\mathcal{B}_n \subset \mathcal{B}'_n$ and $|\mathcal{B}'_n| = (\sqrt{2})^d |\Omega_n|$. Based on Lemma 3.3, it follows that

$$\begin{aligned} \mathbb{P}(X_{n+1} \in \Omega_n^c | X_n = x) &= 1 - \mathbb{P}(X_{n+1} \in \Omega_n | X_n = x) \\ &\geq 1 - \mathbb{P}(X_{n+1} \in \mathcal{B}_n | X_n = x) \\ &\geq \mathbb{P}(X_{n+1} \in \mathcal{B}'_n | X_n = x) - \mathbb{P}(X_{n+1} \in \mathcal{B}_n | X_n = x) = \mathbb{P}(X_{n+1} \in \mathcal{B}'_n \setminus \mathcal{B}_n | X_n = x). \end{aligned}$$

We provide lower-bound estimate for $\mathbb{P}(X_{n+1} \in \mathcal{B}'_n \setminus \mathcal{B}_n | X_n = x)$ as follows.

$$\begin{aligned} \mathbb{P}(X_{n+1} \in \mathcal{B}'_n \setminus \mathcal{B}_n | X_n = x) &= \frac{1}{(\sqrt{2\pi}\sigma_n)^d} \int_{R_n < |y-x^+| \leq \sqrt{2}R_n} \exp \left(-\frac{|y-x^+|^2}{2\sigma_n^2} \right) dy \\ &\geq \frac{|\mathcal{B}'_n| - |\mathcal{B}_n|}{(\sqrt{2\pi}\sigma_n)^d} \exp \left(-\frac{2R_n^2}{2\sigma_n^2} \right) = \beta_1 s_n^d e^{-s_n^2}, \end{aligned}$$

where $s_n = \frac{R_n}{\sigma_n}$ and $\beta_1 = \frac{2^{d/2}-1}{(\sqrt{2\pi c_0})^d}$. It is important to observe that the lower bound is independent of the particular x in Ω_n since we were using the worst-case scenario. Therefore, we have

$$(3.10) \quad \min_{x \in \Omega_n} \mathbb{P}(X_{n+1} \in \Omega_n^c | X_n = x) \geq \beta_1 s_n^d e^{-s_n^2}.$$

By shifting the index from n back to $n-1$, we obtain the target lower bound.

Based on (2.5), we have $\mathbb{P}(A_n^c | A_{n-1}^c) = q_{n-1}(\Omega_n^c) = 1 - |\Omega_n|/|\mathfrak{X}|$ and $\mathbb{P}(B_{n+1} | A_n^c) = q_n(\Omega) = |\Omega|/|\mathfrak{X}|$. From Assumptions **B2** and **B3**, we know that $s_{n-1}^d e^{-s_{n-1}^2}$ and $|\Omega_n|$ both go to zero as $n \rightarrow \infty$. Thus, $\exists M \in \mathbb{N}$ s.t. $\forall n \geq M$,

$$q_{n-1}(\Omega_n^c) = 1 - |\Omega_n|/|\mathfrak{X}| > 1/2 > \beta_1 s_{n-1}^d e^{-s_{n-1}^2},$$

which shows that $\beta_1 s_{n-1}^d e^{-s_{n-1}^2}$ can be a lower bound for both $q_{n-1}(\Omega_n^c)$ and $\min_{x \in \Omega_{n-1}} \mathbb{P}(A_n^c | X_{n-1} = x)$ when $n \geq M$. Finally, we obtain a lower bound for l_{n+1} for any $n \geq M$ as follows.

$$(3.11) \quad l_{n+1} = q_n(\Omega) \min \left(\min_{x \in \Omega_{n-1}} \mathbb{P}(A_n^c | X_{n-1} = x), q_{n-1}(\Omega_n^c) \right) \geq c s_{n-1}^d e^{-s_{n-1}^2},$$

where $c = \beta_1 |\Omega|/|\mathfrak{X}|$, a constant independent of n . \square

We remark that Lemma 3.4 holds under weaker assumptions than **B2-B3**. Consider the assumptions

$$\mathbf{B2'} \quad \lim_{n \rightarrow \infty} s_n = \infty.$$

$$\mathbf{B3'} \quad \lim_{n \rightarrow \infty} |\Omega_n| = 0.$$

Note that **B2-B3** imply **B2'-B3'**, respectively. Lemma 3.4 holds if **B2-B3** are replaced by **B2'-B3'**.

We are ready to present the main lemma showing that the iterates can visit any set of positive Lebesgue measure with high probability.

LEMMA 3.5. *Under the assumptions in **A1**, **A2**, **B2** and **B3**, for any closed subset $\Omega \subseteq \mathfrak{X}$ where $|\Omega| > 0$, we have*

$$(3.12) \quad \lim_{N \rightarrow \infty} \mathbb{P}(\cup_{n=0}^N \{X_n \in \Omega\}) = 1.$$

Proof. Note that all earlier lemmas hold under the set of assumptions. Consider $N \geq 2M$, where M is the positive integer in the proof of Lemma 3.4. Without loss of generality, we assume both M and N to be odd integers. First, we observe that

$$\begin{aligned} \mathbb{P}(\cap_{n=0}^N \{X_n \notin \Omega\}) &= \mathbb{P}(B_0^c \cap B_1^c \cap B_2^c \cap \dots \cap B_{N-1}^c \cap B_N^c) \\ &\leq \mathbb{P}(B_M^c \cap B_{M+2}^c \cap \dots \cap B_{N-2}^c \cap B_N^c) \\ &= \mathbb{P}(B_N^c | B_{N-2}^c \cap \dots \cap B_M^c) \mathbb{P}(B_{N-2}^c \cap \dots \cap B_M^c) \\ &= \mathbb{P}(B_M^c) \prod_{\substack{n=M+1 \\ n \text{ is even}}}^{N-1} \mathbb{P}(B_{n+1}^c | B_{n-1}^c \cap \dots \cap B_M^c) \\ &= \mathbb{P}(B_M^c) \prod_{\substack{n=M+1 \\ n \text{ is even}}}^{N-1} \mathbb{P}(B_{n+1}^c | B_{n-1}^c) \leq \prod_{\substack{n=M-1 \\ n \text{ is even}}}^{N-1} (1 - l_{n+1}), \end{aligned}$$

where we applied the Markov property of the iteration (2.1) in the last equality. We also used results from Lemma 3.1 and Lemma 3.2 to provide upper bounds for the term $\mathbb{P}(B_M^c)$ and the conditional probabilities $\{\mathbb{P}(B_{n+1}^c | B_{n-1}^c)\}$ for all even integer n from $M+1$ to $N-1$.

Applying [Lemma 3.4](#) and Assumption [B2](#), we have $l_{n+1} \geq c \frac{(\log(n-1))^{d/2}}{n-1}$ for $n \geq M$. Thus,

$$(3.13) \quad \log(1 - l_{n+1}) \leq -l_{n+1} \leq -\frac{c(\log(n-1))^{d/2}}{n-1} \leq -\frac{c}{n-1}, \quad n \geq \max(4, M).$$

Therefore, we have

$$(3.14) \quad \lim_{N \rightarrow \infty} \mathbb{P}(\cap_{n=0}^N \{X_n \notin \Omega\}) \leq \lim_{N \rightarrow \infty} \exp\left(\sum_{\substack{n=M-1 \\ n \text{ is even}}}^{N-1} \log(1 - l_{n+1})\right) = 0,$$

which is equivalent to [\(3.12\)](#). \square

Again, we remark that [Lemma 3.5](#) holds if we replace [B3](#) by a weaker assumption [B3'](#).

3.2. Property Two: Jumping-In Easier Than Jumping-Out. In [Subsection 3.1](#), we have shown that the iterates $\{X_n\}$ visit any subset of \mathfrak{X} of a positive Lebesgue measure with high probability. Next, we will show that under the assumptions stated in [Section 2](#), the iterate X_n is more likely to jump from Ω_n^c into the set Ω_{n+1} than to jump from Ω_n to Ω_{n+1}^c . That is,

$$(3.15) \quad \lim_{n \rightarrow \infty} \frac{\mathbb{P}(X_{n+1} \in \Omega_{n+1}^c | X_n \in \Omega_n)}{\mathbb{P}(X_{n+1} \in \Omega_{n+1} | X_n \in \Omega_n^c)} = \lim_{n \rightarrow \infty} \frac{p_n(\Omega_{n+1}^c)}{q_n(\Omega_{n+1})} = 0.$$

This is a necessary property for the SGD algorithm in [\(2.1\)](#) to guarantee global convergence. While $q_n(\Omega_{n+1}) = \frac{|\Omega_{n+1}|}{|\mathfrak{X}|}$ is given explicitly, we will use an upper bound for $p_n(\Omega_{n+1}^c)$ in the following lemmas. The technique here is different from those in [Subsection 3.1](#) where a lower bound of $p_n(\Omega_{n+1}^c)$ was used.

Consider x as a realization of the random variable X_n . Recall $x^+ = x - \eta_n G(x)$ as used in [\(2.3\)](#). First, we justify that for large n , $x^+ \in \Omega_{n+1}$ if $x \in \Omega_n$ as a realization of X_n .

LEMMA 3.6. *Under the assumptions in [A1-A2](#), [B1](#) and [B3](#), for any $\gamma > \gamma^* = (2\eta b_2 - \eta^2 b_2^2)^{-1}$, we choose $\epsilon > 0$ sufficiently small so that $B(x^*; \epsilon) \subseteq \Omega_{sc}$ and*

$$(3.16) \quad b_\gamma \nabla^2 f(x^*) \leq \nabla^2 f(z) \leq b_\gamma^{-1} \nabla^2 f(x^*), \quad b_\gamma = \left(1 - \frac{b_1}{\gamma b_2}\right)^{1/2} \leq 1,$$

for all $z \in B(x^*; \epsilon)$, where the inequalities hold entry-wise. Then, $\exists N \in \mathbb{N}$ such that $\forall n \geq N$, $\Omega_n \subset B(x^*; \epsilon)$. Moreover, if $x \in \Omega_n$ and $n > N$, then $x^+ = x - \eta_n G(x) \in \Omega_{n+1}$.

Proof. Consider our global minimizer x^* and its ϵ -neighborhood $B(x^*; \epsilon)$ with the given ϵ . By construction, the sequence $\{f_n\}$ contains the scalar cutoff values in [\(2.1\)](#). By [B3](#), the volume of the sublevel set Ω_n determined by f_n decays to 0 as n increases, so we have $\lim_{n \rightarrow \infty} f_n = f(x^*) = f^*$. Thus, $\exists N_1 \in \mathbb{N}$ such that for any $n \geq N_1$, $\Omega_n \subset B(x^*; \epsilon) \subseteq \Omega_{sc}$. Next, we consider $x \in \Omega_n$ for $n > N_1$ such that $\Omega_n \subseteq \Omega_{n-1} \subset B(x^*; \epsilon)$.

Based on Assumptions [A1-A2](#), the following holds for any $y_1, y_2 \in \Omega_{sc}$.

$$\mathbf{C1} \quad G(y_1)^T(y_2 - y_1) + b_1/2|y_2 - y_1|_2^2 \leq f(y_2) - f(y_1) \leq G(y_1)^T(y_2 - y_1) + b_2/2|y_2 - y_1|_2^2.$$

$$\mathbf{C2} \quad \sqrt{2b_1(f(y_1) - f^*)} \leq |G(y_1)| \leq \sqrt{2b_2(f(y_1) - f^*)}, \text{ with } f^* = f(x^*).$$

Here $|\cdot|_2$ denotes the Euclidean (ℓ^2) norm of the vector. We plug $y_1 = x$ and $y_2 = x^+ = x - \eta_n G(x)$ into [C1](#) and [C2](#). Since $0 < \eta_n = \eta < 2/b_2$ (by Assumption [B1](#)), we have $\eta - b_2\eta^2/2 > 0$ and

$$(3.17) \quad \begin{aligned} f(x^+) - f^* &\leq f(x) - f^* - (\eta - b_2\eta^2/2) |G(x)|^2 \\ &\leq (f(x) - f^*) \left(1 - 2\eta b_1 + \eta^2 b_1 b_2\right) = (f(x) - f^*) \left(1 - \frac{b_1}{\gamma^* b_2}\right), \end{aligned}$$

where $\gamma^* = (2\eta b_2 - \eta^2 b_2^2)^{-1} = (1 - (\eta b_2 - 1)^2)^{-1} \geq 1$ as a result of $0 < \eta < 2/b_2$. If $x \in \Omega_{n+1} \subseteq \Omega_n$, [\(3.17\)](#) also implies $x^+ \in \Omega_{n+1}$ since $f(x^+) < f(x) \leq f_{n+1}$. Therefore, we focus on the case where $x \in \Omega_n \setminus \Omega_{n+1}$. The set difference is non-empty since $|\Omega_{n+1}| < |\Omega_n|$ by Assumption [B3](#).

From the Taylor expansion of f around x^* and the multi-dimensional mean-value theorem, $\forall y \in B(x^*; \epsilon)$, we have

$$f(y) = f(x^*) + \nabla f(x^*)^\top (y - x^*) + \frac{1}{2}(y - x^*)^\top \nabla^2 f(z(y))(y - x^*), \quad z(y) = \tau x^* + (1 - \tau)y,$$

for some $0 \leq \tau \leq 1$. Since $y \in B(x^*; \epsilon)$, we also have that $z(y) \in B(x^*; \epsilon)$. Moreover, as a result of $\nabla f(x^*) = 0$ and $f(x^*) = \mathfrak{f}^*$, together with (3.16), $\forall y \in B(x^*; \epsilon)$, we have

$$(3.18) \quad \frac{b_\gamma}{2}(y - x^*)^\top \nabla^2 f(x^*)(y - x^*) \leq f(y) - \mathfrak{f}^* \leq \frac{1}{2b_\gamma}(y - x^*)^\top \nabla^2 f(x^*)(y - x^*).$$

Next, we restrict y to $\Omega_{n-1} \setminus \Omega_n$, $\forall n > N_1$, a subset of $B(x^*; \epsilon)$. The set difference is non-empty since $|\Omega_n| < |\Omega_{n-1}|$ by **B3**. Using the fact that $f_n < f(y) \leq f_{n-1}$ and (3.18), we obtain that

$$(3.19) \quad \Omega_{n-1} \setminus \Omega_n \subseteq \overline{E}_{n-1} \setminus \underline{E}_n,$$

where the two sets \overline{E}_{n-1} and \underline{E}_n are two nested ellipsoids defined by

$$\begin{aligned} \overline{E}_n &:= \{x | (x - x^*)^\top \nabla^2 f(x^*)(x - x^*) \leq 2b_\gamma^{-1}(f_n - \mathfrak{f}^*)\}, \\ \underline{E}_n &:= \{x | (x - x^*)^\top \nabla^2 f(x^*)(x - x^*) \leq 2b_\gamma(f_n - \mathfrak{f}^*)\}. \end{aligned}$$

We then have the important set relation for any $n > N_1$,

$$(3.20) \quad \underline{E}_n \subseteq \Omega_n \subseteq \Omega_{n-1} \subseteq \overline{E}_{n-1}, \quad \underline{E}_{n+1} \subseteq \Omega_{n+1} \subseteq \Omega_n \subseteq \overline{E}_n.$$

Combining the two set relations, we have

$$(3.21) \quad \underline{E}_n \subseteq \Omega_n \subseteq \overline{E}_n, \quad n > N_1.$$

In other words, Ω_n is nested between two ellipsoids centered at x^* for $n > N_1$. Its volume is thus bounded in between by $|\underline{E}_n|$ and $|\overline{E}_n|$. Define $c_3 = (\sqrt{2}c_0^{-1})^d / \sqrt{\det(\nabla^2 f(x^*))}$, we have

$$(3.22) \quad |\underline{E}_n| = c_3 b_\gamma^{d/2} (f_n - \mathfrak{f}^*)^{d/2} \leq |\Omega_n| \leq c_3 b_\gamma^{-d/2} (f_n - \mathfrak{f}^*)^{d/2} = |\overline{E}_n|,$$

$$(3.23) \quad b_\gamma c_3^{-2/d} |\Omega_n|^{2/d} \leq f_n - \mathfrak{f}^* \leq b_\gamma^{-1} c_3^{-2/d} |\Omega_n|^{2/d},$$

for $n > N_1$. Based on Assumption **B3**, for $n \geq 1$, $|\Omega_{n+1}| = |\Omega_0|n^{-\alpha}$ for some $\alpha \in (0, 1)$. Together with (3.23), we have the following for $n > \max(2, N_1)$,

$$(3.24) \quad b_n \leq \frac{f_{n+1} - \mathfrak{f}^*}{f_n - \mathfrak{f}^*} \leq 1, \quad \text{where } b_n = b_\gamma^2 \left(\frac{n}{n-1} \right)^{-\frac{2\alpha}{d}} = \left(1 - \frac{b_1}{\gamma b_2} \right) \left(1 - \frac{1}{n} \right)^{\frac{2\alpha}{d}}.$$

On the other hand, since $\gamma > \gamma^* \geq 1$, we know that $b_\gamma > b_{\gamma^*}$ based on (3.16). Therefore, let N_2 be the smallest integer that is not smaller than $\left(1 - (b_{\gamma^*}/b_\gamma)^{\frac{d}{\alpha}} \right)^{-1}$. Then $\forall n \geq N_2$, we have $b_n \geq 1 - \frac{b_1}{\gamma^* b_2}$. Together with (3.17), we find that

$$(3.25) \quad \frac{f(x^+) - \mathfrak{f}^*}{f_n - \mathfrak{f}^*} \leq \frac{f(x^+) - \mathfrak{f}^*}{f(x) - \mathfrak{f}^*} \leq 1 - \frac{b_1}{\gamma^* b_2} \leq b_n \leq \frac{f_{n+1} - \mathfrak{f}^*}{f_n - \mathfrak{f}^*}, \quad \forall n \geq N = \max(N_1, N_2).$$

Since (3.25) also implies $f(x^+) \leq f_{n+1}$, we conclude that $x^+ \in \Omega_{n+1}$ provided $x \in \Omega_n$. \square

Next, we provide a lower bound for $\frac{d_n(x)}{c_0 \sqrt[d]{|\Omega_n|}}$, where

$$(3.26) \quad d_n(x) = \inf_{y \in \Omega_{n+1}^c} |y - x^+|$$

for a given $x \in \Omega_n$ and $x^+ = x - \eta_n G(x)$.

LEMMA 3.7. *Let Assumption **B2** and all conditions in Lemma 3.6 hold. There exists $N_3 \in \mathbb{N}$ such that $\forall n \geq N_3$, we have $c^* \leq \frac{d_n(x)}{c_0 \sqrt[d]{|\Omega_n|}} \leq 1$ for all $x \in \Omega_n$, where $c^* = \frac{1}{4\gamma^*} \left(\frac{b_1}{b_2}\right)^{\frac{3}{2}}$ and $\gamma^* = (2\eta b_2 - \eta^2 b_2^2)^{-1}$.*

Proof. Let N, γ be those given in the conditions of Lemma 3.6, whose conclusions hold here by the assumptions. We consider the case that $x \in \Omega_n$ where $n > N$. Here, x is a possible realization of the random variable X_n . Thus, we have $x^+ \in \Omega_{n+1}$ and $\Omega_{n+1} \subseteq \Omega_{sc}$. We also have that

$$d_n(x) = \inf_{y \in \Omega_{n+1}^c} |y - x^+| = \inf_{y \in \partial\Omega_{n+1}^c} |y - x^+| = \inf_{y \in \partial\Omega_{n+1}} |y - x^+|.$$

See Figure 1b for an illustration of x^+ , $d_n(x)$ and Ω_{n+1} . Consider a ball $B(x^+; d_n(x))$ centered at x^+ with a radius $d_n(x)$. Since $B(x^+; d_n(x)) \subseteq \Omega_{n+1} \subseteq \Omega_n$, $|B(x^+; d_n(x))| \leq |\Omega_n|$, or equivalently, $d_n(x)/R_n = d_n(x)/(c_0 \sqrt[d]{|\Omega_n|}) \leq 1$, where R_n is defined in the proof for Lemma 3.4. Thus, we have the upper bound for $d_n(x)$.

Combining **C1** and **C2** in Lemma 3.6, we find that

$$(3.27) \quad f(y_2) - f(y_1) \leq \sqrt{2b_2(f(y_1) - f^*)} |y_2 - y_1| + b_2/2 |y_2 - y_1|^2$$

$$(3.28) \quad = (\sqrt{b_2/2} |y_2 - y_1| + \sqrt{f(y_1) - f^*})^2 - (f(y_1) - f^*),$$

which implies that for any $y_1, y_2 \in \Omega_{sc}$, we have

$$(3.29) \quad |y_2 - y_1| \geq \sqrt{2/b_2} (\sqrt{f(y_2) - f^*} - \sqrt{f(y_1) - f^*}).$$

By plugging $y_1 = x^+$ and any $y_2 \in \partial\Omega_{n+1}$ into (3.29) (note that $y_1, y_2 \in \Omega_{sc}$), we have that

$$(3.30) \quad d_n(x) \geq \sqrt{\frac{2}{b_2}} \inf_{y_2 \in \partial\Omega_{n+1}} (\sqrt{f(y_2) - f^*} - \sqrt{f(x^+) - f^*}) = \sqrt{\frac{2}{b_2}} (\sqrt{f_{n+1} - f^*} - \sqrt{f(x^+) - f^*}).$$

Combining (3.30) with the right-hand side of (3.22) in Lemma 3.6, we have

$$(3.31) \quad \begin{aligned} \frac{d_n(x)}{c_0 \sqrt[d]{|\Omega_n|}} &\geq \frac{\sqrt{2/b_2} (\sqrt{f_{n+1} - f^*} - \sqrt{f(x^+) - f^*})}{c_0 b_\gamma^{-\frac{1}{2}} (c_3)^{\frac{1}{d}} \sqrt{f_n - f^*}} \\ &\geq \frac{\sqrt{2/b_2} \left(1 - \frac{b_1}{\gamma b_2}\right)^{\frac{1}{4}}}{\sqrt{2/b_1}} \left(\sqrt{b_n} - \sqrt{\frac{f(x^+) - f^*}{f_n - f^*}}\right) \\ &> \sqrt{\frac{b_1}{b_2}} \sqrt{1 - \frac{b_1}{\gamma b_2}} \left(\sqrt{1 - \frac{b_1}{\gamma b_2}} \left(1 - \frac{1}{n}\right)^{\frac{\alpha}{d}} - \sqrt{1 - \frac{b_1}{\gamma^* b_2}}\right). \end{aligned}$$

Here, we have applied (3.25) in Lemma 3.6 and the fact that $c_3 = (\sqrt{2}c_0^{-1})^d / \sqrt{\det(\nabla^2 f(x^*))} \leq (\sqrt{2/b_1}c_0^{-1})^d$ by **A1-A2**. Note that the last term of (3.31) depends on both γ and n , but it no longer depends on the position of $x \in \Omega_n$. Moreover,

$$\lim_{\gamma \rightarrow \infty} \lim_{n \rightarrow \infty} \sqrt{1 - \frac{b_1}{\gamma b_2}} \left(\sqrt{1 - \frac{b_1}{\gamma b_2}} \left(1 - \frac{1}{n}\right)^{\frac{\alpha}{d}} - \sqrt{1 - \frac{b_1}{\gamma^* b_2}}\right) = 1 - \sqrt{1 - \frac{b_1}{\gamma^* b_2}}.$$

If we set $\gamma = 4\gamma^*$, let N to be the corresponding integer in Lemma 3.6 for this γ , and choose $N_3 > N$ such that $b_n \geq 1 - \frac{b_1}{2\gamma^* b_2}$ (since $\lim_{n \rightarrow \infty} b_n = 1 - \frac{b_1}{\gamma b_2} = 1 - \frac{b_1}{4\gamma^* b_2}$), then $\forall n \geq N_3$, (3.31) leads to

$$(3.32) \quad \frac{d_n(x)}{c_0 \sqrt[d]{|\Omega_n|}} \geq \sqrt{\frac{b_1}{b_2}} \sqrt{1 - \frac{b_1}{4\gamma^* b_2}} \left(\sqrt{1 - \frac{b_1}{2\gamma^* b_2}} - \sqrt{1 - \frac{b_1}{\gamma^* b_2}}\right) \geq \frac{1}{4\gamma^*} \left(\frac{b_1}{b_2}\right)^{\frac{3}{2}} := c^*. \quad \square$$

Remark 3.8. In the proof above, we applied [Lemma 3.6](#) by setting $\gamma = 4\gamma^*$. However, γ can be chosen arbitrarily large, and the lower bound c^* can consequently be made bigger by a constant factor. As γ increases, the positive integer N in both [Lemma 3.6](#) and [Lemma 3.7](#) must correspondingly increase.

Remark 3.9. So far, we have used Assumption [B3](#) to simplify the proof. However, the assumption can be relaxed to, for example, $|\Omega_n| = \mathcal{O}(n^{-\alpha})$ such that $C_1 n^{-\alpha} \leq |\Omega_n| \leq C_2 n^{-\alpha}$ for some constants $C_1, C_2 > 0$ when n is large enough. In such cases, [\(3.32\)](#) still holds but with a different constant c^* .

The proof of [Lemma 3.7](#) relies on Assumption [B1](#) that the step size η_n is a constant as n goes to infinity. We choose $\eta_n = \eta < 2/b_2$ as required for the convergence of the gradient descent algorithm applied to a convex optimization problem. Note that [B1](#) requires the knowledge or an estimation of b_2 , also known as the Lipschitz constant of the gradient function $G(x)$ over Ω_{sc} (see Assumption [A1](#)).

If we only aim for convergence but not necessarily an algebraic order of convergence, we can relax Assumption [B1](#) by assuming $\lim_{n \rightarrow \infty} \eta_n = 0$, which drops the requirement of estimating b_2 . For example, we may replace [B1-B3](#) by the following set of assumptions.

B1 The step size in [\(2.1\)](#) satisfies $\eta_n = \mathcal{O}\left(\frac{1}{\log(\log n)}\right)$.

B2 For $n \geq 1$, $\sigma_n = \frac{c_0 \sqrt[d]{|\Omega_n|}}{\sqrt{\log n}}$.

B3 $|\Omega_n| = \mathcal{O}\left(\frac{1}{\log n}\right)$ based on the properly chosen $\{f_n\}$.

Under Assumptions [B1-B3](#), [\(3.15\)](#) still holds, but we will no longer have the algebraic-rate estimation for the upper and lower bounds stated in [Lemma 3.10](#) below. As a result, the algebraic convergence in [Theorem 2.1](#) is replaced by a slower logarithmic convergence.

We will see the fact that $d_n(x)/\sqrt[d]{|\Omega_n|}$ is bounded below by a constant independent of both n and x is the key to obtaining an algebraic rate of convergence. Next, we combine results from [Lemma 3.6](#) and [Lemma 3.7](#) to show [\(3.15\)](#) holds.

LEMMA 3.10. *Under the assumptions [A1-A2](#) and [B1-B3](#), we define $\kappa := |\Omega_0|/|\mathfrak{X}|$. Then we have*

$$(3.33) \quad q_n(\Omega_{n+1}) = \kappa n^{-\alpha}, \quad \forall n \geq 1.$$

Moreover, there exists $N \in \mathbb{N}$ such that

$$(3.34) \quad \beta_1 n^{-1} \leq p_n(\Omega_{n+1}^c) \leq \beta_2 n^{-\alpha_2}, \quad \forall n \geq N,$$

where $\alpha_2 = \frac{(c^*)^2}{4} + \frac{\alpha}{2}$, $\beta_1 = \frac{2^{d/2}-1}{(\sqrt{2\pi}c_0)^d}$ and $\beta_2 = 1$. In particular, if $0 < \alpha < \frac{(c^*)^2}{2}$, then [\(3.15\)](#) holds.

Proof. Based on [\(2.5\)](#), we have $\frac{q_n(\Omega_{n+1})}{|\Omega_{n+1}|} = \frac{1}{|\mathfrak{X}|}$ so [\(3.33\)](#) follows directly from [B3](#). To prove that [\(3.15\)](#) holds when $0 < \alpha < \frac{(c^*)^2}{2}$, we show that $\lim_{n \rightarrow \infty} \frac{p_n(\Omega_{n+1}^c)}{|\Omega_{n+1}|} = 0$. Based on [\(2.3\)-\(2.4\)](#), we have

$$p_n(\Omega_{n+1}^c) = \frac{\int_{\Omega_n} \left(\int_{\Omega_{n+1}^c} k_n(y, x) dy \right) d\mu_n(x)}{\int_{\Omega_n} d\mu_n(x)} \leq \max_{x \in \Omega_n} \int_{\Omega_{n+1}^c} k_n(y, x) dy.$$

For $n > N_3$ where N_3 is the positive integer in the statement and the proof for [Lemma 3.7](#), we have $x^+ \in \Omega_{n+1}$ provided that $x \in \Omega_n$. In this case, we also have $B(x^+; d_n(x)) \subseteq \Omega_{n+1}$ where $d_n(x) = \inf_{y \in \Omega_{n+1}^c} |y - x^+|$ (see [\(3.26\)](#)). We then have

$$\max_{x \in \Omega_n} \int_{\Omega_{n+1}^c} k_n(y, x) dy \leq \max_{x \in \Omega_n} \frac{1}{(\sqrt{2\pi}\sigma_n)^d} \int_{|y-x^+| > d_n(x)} \exp\left(-\frac{|y-x^+|^2}{2\sigma_n^2}\right) dy = \max_{x \in \Omega_n} \mathbb{P}\left(Q > \frac{d_n(x)^2}{\sigma_n^2}\right),$$

where the random variable $Q \sim \chi_d^2$, the chi-squared distribution (a sum of the squares of d independent standard normal random variables). Based on **B2** and **Lemma 3.7**, for any $x \in \Omega_n$,

$$(3.35) \quad c^* \sqrt{\log n} \leq \frac{d_n(x)}{\sigma_n} = \frac{d_n(x) \sqrt{\log n}}{c_0 \sqrt[d]{|\Omega_n|}} \leq \sqrt{\log n}, \quad \forall n \geq N_3.$$

Therefore, we have

$$(3.36) \quad p_n(\Omega_{n+1}^c) \leq \max_{x \in \Omega_n} \int_{\Omega_{n+1}^c} k_n(y, x) dy \leq \max_{x \in \Omega_n} \mathbb{P} \left(Q > \frac{d_n(x)^2}{\sigma_n^2} \right) \leq \mathbb{P} (Q > (c^*)^2 \log n),$$

where we dropped “ $\max_{x \in \Omega_n}$ ” in the last term of (3.36) since the final upper bound is x -independent.

Based on the properties of the chi-squared distribution, we have the following bounds for different d .

- When $d = 1$, and thus $Q = Z^2$ where $Z \sim \mathcal{N}(0, 1)$, we have the Chernoff bound [6, Eqn.(5)]

$$(3.37) \quad \mathbb{P} (Q > (c^*)^2 \log n) = 2\mathbb{P} (Z > c^* \sqrt{\log n}) = \operatorname{erfc} \left(\frac{c^* \sqrt{\log n}}{\sqrt{2}} \right) \leq e^{-(c^*)^2 (\log n)/2} = n^{-\frac{(c^*)^2}{2}},$$

where $\operatorname{erfc}(\cdot)$ is the complementary error function.

- The cumulative distribution function of the chi-squared distribution is $F(x) = \frac{\gamma(\frac{d}{2}, \frac{x}{2})}{\Gamma(\frac{d}{2})}$ where $\gamma(a, z)$ is the lower incomplete gamma function. When $d = 2$, it is well known that $F(x)$ has an analytic form $1 - e^{-x/2}$, and thus

$$(3.38) \quad \mathbb{P} (Q > (c^*)^2 \log n) = e^{-(c^*)^2 (\log n)/2} = n^{-\frac{(c^*)^2}{2}}.$$

- When $a > 1$ and $z > 2(a - 1)$ where $z \in \mathbb{R}$, there exists an upper bound for the upper incomplete function $\Gamma(a, z) = \Gamma(a) - \gamma(a, z)$ as $\Gamma(a, z) < 2z^{a-1}e^{-z}$ [18, Eqn.(3.2)]. Based on (3.35), there exists $N_4 \in \mathbb{N}$ such that $\forall n \geq \max(N_3, N_4)$, $(c^*)^2 (\log n)/2 > d - 2$. When $d \geq 3$, by plugging in $a = \frac{d}{2}$ and $z = (c^*)^2 (\log n)/2$, we obtain

$$(3.39) \quad \mathbb{P} (Q > (c^*)^2 (\log n)) < \frac{2 \left((c^*)^2 (\log n)/2 \right)^{\frac{d}{2}-1}}{\Gamma(\frac{d}{2})} e^{-\frac{(c^*)^2 \log n}{2}} = \frac{2^{2-\frac{d}{2}}}{\Gamma(\frac{d}{2})} \left((c^*)^2 \log n \right)^{\frac{d}{2}-1} n^{-\frac{(c^*)^2}{2}}.$$

Thus, (3.39) holds if the dimension $d \geq 3$ and $n \geq \max(N_3, N_4)$. Here, N_4 is d -dependent.

These three scenarios cover all possible d , the number of dimensions. Combining all the cases above with **B2-B3** and (3.35), we have

$$(3.40) \quad \frac{p_n(\Omega_{n+1}^c)}{|\Omega_{n+1}|} \leq \begin{cases} \frac{1}{|\Omega_0|} n^{\alpha - (c^*)^2/2}, & d = 1, 2, \\ \frac{2^{2-d/2}}{|\Omega_0| \Gamma(\frac{d}{2})} (\log n)^{\frac{d}{2}-1} n^{\alpha - (c^*)^2/2}, & d \geq 3. \end{cases}$$

Therefore, if we choose $0 < \alpha < \frac{(c^*)^2}{2}$, (3.15) holds. Also, there exists $N_5 \in \mathbb{N}$ such that $\forall n \geq N := \max\{N_3, N_4, N_5\}$, we have $2(\log n)^{\frac{d}{2}-1} < n^{(c^*)^2/4 - \alpha/2}$. Since $\frac{(c^*)^2}{4} + \frac{\alpha}{2} < \frac{(c^*)^2}{2}$, and $2^{1-d/2} < \Gamma(\frac{d}{2})$ for $d \geq 3$, we can now integrate our results for different values of d and obtain an upper bound

$$(3.41) \quad p_n(\Omega_{n+1}^c) \leq n^{-(c^*)^2/4 - \alpha/2}.$$

The lower bound in (3.34) is based on (3.10) and **B3**. □

3.3. Proof of the Main Theorem. Once we have both [Lemma 3.5](#) and [Lemma 3.10](#), in particular, the upper and lower bounds for $p_n(\Omega_{n+1}^c) = \mathbb{P}(X_{n+1} \in \Omega_{n+1}^c | X_n \in \Omega_n)$, we are ready to prove our main result. [Theorem 2.1](#) demonstrates that the iterates $\{X_n\}$ converge to x^* in probability. That is,

$$(3.42) \quad \lim_{n \rightarrow \infty} \mathbb{P}(|X_n - x^*| > \epsilon) = 0, \quad \forall \epsilon > 0.$$

Proof of Theorem 2.1. Since [A1-A2](#) and [B1-B3](#) hold, results from all previous lemmas apply.

Recall that A_n denotes the event $\{X_n \in \Omega_n\}$. We consider $n \geq N$ where N is the integer in [Lemma 3.10](#) such that [\(3.34\)](#) holds. By the law of total probability,

$$(3.43) \quad \begin{aligned} \mathbb{P}(A_{n+1}^c) &= \mathbb{P}(A_{n+1}^c | A_n) \mathbb{P}(A_n) + \mathbb{P}(A_{n+1}^c | A_n^c) \mathbb{P}(A_n^c) \\ &\leq \beta_2 n^{-\alpha_2} (1 - \mathbb{P}(A_n^c)) + (1 - \kappa n^{-\alpha}) \mathbb{P}(A_n^c) \\ &= g(n) \mathbb{P}(A_n^c) + h(n), \end{aligned}$$

where $0 < \alpha < \alpha_2 < \frac{(c^*)^2}{2} < 1$, $g(n) = 1 - \kappa n^{-\alpha} - \beta_2 n^{-\alpha_2}$ and $h(n) = \beta_2 n^{-\alpha_2}$.

Consider the following first-order non-homogeneous recurrence with variable coefficients

$$r_{n+1} = g(n)r_n + h(n)$$

starting with $n = n_0$ and $r_{n_0} = \mathbb{P}(A_{n_0}^c)$, where $n_0 = \min\{n \in \mathbb{N} | n \geq N, g(n) > 0\}$. Based on [\(3.43\)](#), $\mathbb{P}(A_n^c) \leq r_n, \forall n \geq n_0$, because $g(n)$ is monotonically increasing and $g(n_0) > 0$. Thus, it is sufficient to show that $\lim_{n \rightarrow \infty} r_n = 0$, which directly implies $\lim_{n \rightarrow \infty} \mathbb{P}(A_n^c) = 0$.

The recurrence $\{r_n\}$ has an analytic solution [[20](#), Section 3.3]. That is,

$$\begin{aligned} r_n &= \left(\prod_{k=n_0}^{n-1} g(k) \right) \left(r_{n_0} + \sum_{m=n_0}^{n-1} \frac{h(m)}{\prod_{k=n_0}^m g(k)} \right) \\ &= \left(\prod_{k=n_0}^{n-1} (1 - \kappa k^{-\alpha} - \beta_2 k^{-\alpha_2}) \right) \left(r_{n_0} + \sum_{m=n_0}^{n-1} \frac{\beta_2 m^{-\alpha_2}}{\prod_{k=n_0}^m (1 - \kappa k^{-\alpha} - \beta_2 k^{-\alpha_2})} \right) \\ &= \underbrace{r_{n_0} \left(\prod_{k=n_0}^{n-1} (1 - \kappa k^{-\alpha} - \beta_2 k^{-\alpha_2}) \right)}_{I_1(n)} + \underbrace{\beta_2 \sum_{m=n_0}^{n-1} m^{-\alpha_2} \prod_{k=m+1}^{n-1} (1 - \kappa k^{-\alpha} - \beta_2 k^{-\alpha_2})}_{I_2(n)}. \end{aligned}$$

Note that for any $k_0 \in \mathbb{N}$,

$$(3.44) \quad \begin{aligned} \sum_{k=k_0}^{n-1} \log(1 - \kappa k^{-\alpha} - \beta_2 k^{-\alpha_2}) &\leq - \sum_{k=k_0}^{n-1} (\kappa k^{-\alpha} + \beta_2 k^{-\alpha_2}) \leq - \int_{k_0}^n (\kappa x^{-\alpha} + \beta_2 x^{-\alpha_2}) dx \\ &= \frac{\kappa (k_0^{1-\alpha} - n^{1-\alpha})}{1-\alpha} + \frac{\beta_2 (k_0^{1-\alpha_2} - n^{1-\alpha_2})}{1-\alpha_2}. \end{aligned}$$

With $z_1 := \frac{\kappa}{1-\alpha}$ and $z_2 := \frac{\beta_2}{1-\alpha_2}$, we have the following by plugging $k_0 = n_0$ into [\(3.44\)](#).

$$\lim_{n \rightarrow \infty} I_1(n) \leq r_{n_0} \exp(z_1 n_0^{1-\alpha}) \exp(z_2 n_0^{1-\alpha_2}) \lim_{n \rightarrow \infty} \exp(-z_1 n^{1-\alpha} - z_2 n^{1-\alpha_2}) = 0.$$

We remark that $I_1(n)$ decays to zero exponentially.

Next, we will provide an asymptotic decay rate for $I_2(n)$. Plugging $k_0 = m+1$ into [\(3.44\)](#),

$$\begin{aligned} I_2(n) &\leq \beta_2 e^{-z_1 n^{1-\alpha}} e^{-z_2 n^{1-\alpha_2}} \sum_{m=n_0}^{n-1} m^{-\alpha_2} e^{z_1 (m+1)^{1-\alpha}} e^{z_2 (m+1)^{1-\alpha_2}} \\ &\leq \underbrace{\beta_2 e^{-z_1 n^{1-\alpha}} e^{-z_2 n^{1-\alpha_2}} \int_{n_0}^n s^{-\alpha_2} e^{z_1 (s+1)^{1-\alpha}} e^{z_2 (s+1)^{1-\alpha_2}} ds}_{K(n)}. \end{aligned}$$

We denote the right-hand side of the last inequality as $K(n)$. Consider $Z(n) = \beta_2 \kappa^{-1} n^{\alpha-\alpha_2}$. We may generalize $Z(n)$ and $K(n)$ to functions $Z(x)$ and $K(x)$. Using L'Hospital's rule,

$$\begin{aligned} \lim_{n \rightarrow \infty} \frac{K(n)}{Z(n)} &= \lim_{x \rightarrow \infty} \frac{K(x)}{Z(x)} \\ &= \lim_{x \rightarrow \infty} \frac{\beta_2 \int_{n_0}^x s^{-\alpha_2} e^{z_1(s+1)^{1-\alpha}} e^{z_2(s+1)^{1-\alpha_2}} ds}{(\beta_2 \kappa^{-1} x^{\alpha-\alpha_2}) e^{z_1 x^{1-\alpha}} e^{z_2 x^{1-\alpha_2}}} \\ &= \lim_{x \rightarrow \infty} \frac{\kappa x^{-\alpha_2} e^{z_1(x+1)^{1-\alpha}} e^{z_2(x+1)^{1-\alpha_2}}}{x^{\alpha-\alpha_2} e^{z_1 x^{1-\alpha}} e^{z_2 x^{1-\alpha_2}} ((\alpha - \alpha_2)x^{-1} + z_1(1-\alpha)x^{-\alpha} + z_2(1-\alpha_2)x^{-\alpha_2})} \\ &= \lim_{x \rightarrow \infty} \frac{\kappa x^{-\alpha}}{(\alpha - \alpha_2)x^{-1} + \kappa x^{-\alpha} + \beta_2 x^{-\alpha_2}} \lim_{x \rightarrow \infty} \frac{e^{z_1(x+1)^{1-\alpha}}}{e^{z_1 x^{1-\alpha}}} \lim_{x \rightarrow \infty} \frac{e^{z_2(x+1)^{1-\alpha_2}}}{e^{z_2 x^{1-\alpha_2}}} = 1. \end{aligned}$$

We have just proved that $K(n) \sim \beta_2 \kappa^{-1} n^{\alpha-\alpha_2}$. Thus, $r_n = \mathcal{O}(n^{\alpha-\alpha_2})$ and $\lim_{n \rightarrow \infty} r_n = 0$.

Based on (3.21), the sublevel set Ω_n is contained in a slightly bigger ellipsoid \bar{E}_n , which is further contained in a ball centered at x^* with a radius $\sqrt{2(f_n - \bar{f}^*)/b_1}$ [1, P. 462]. Meanwhile, (3.23) provides an upper bound $\sqrt{f_n - \bar{f}^*} \leq \mathbf{c} n^{-\alpha/d}$ where $\mathbf{c}^d = b_\gamma^{-1/2} c_3^{-1} |\mathfrak{X}|$. Thus, with $\mathbf{c}_1 := \sqrt{2/b_1} \mathbf{c}$, we have

$$(3.45) \quad |x - x^*| \leq \sqrt{2(f_n - \bar{f}^*)/b_1} \leq \mathbf{c}_1 n^{-\alpha/d}, \quad \forall x \in \Omega_n.$$

For $n \geq n_1$ where $n_1 = \min\{n \in \mathbb{N} | n \geq n_0, I_1(n) < I_2(n), K(n) < 2Z(n)\}$, we have

$$(3.46) \quad \mathbb{P}(X_n \notin \Omega_n) = \mathbb{P}(A_n^c) \leq r_n < 2I_2(n) \leq 4\beta_2 \kappa^{-1} n^{\alpha-\alpha_2} = \mathbf{c}_2 n^{\alpha-\alpha_2}, \quad \mathbf{c}_2 := 4\beta_2 \kappa^{-1}.$$

Next, we combine (3.45) and (3.46). Given $\epsilon > 0$, $\forall n \geq \mathcal{N}_1 = \max(n_1, \lceil (\epsilon \mathbf{c}_1^{-1})^{-d/\alpha} \rceil)$,

$$\mathbb{P}(|X_n - x^*| > \epsilon) \leq \mathbb{P}(|X_n - x^*| > \mathbf{c}_1 n^{-\alpha/d}) \leq \mathbb{P}(X_n \notin \Omega_n) \leq \mathbf{c}_2 n^{\alpha-\alpha_2},$$

which indicates convergence of the iterates $\{X_n\}$ in probability (3.42).

Similarly, given any $\delta > 0$, for all $n \geq \mathcal{N}_2 = \max(n_1, \lceil (\delta \mathbf{c}_2^{-1})^{\alpha_2-\alpha} \rceil)$, we have

$$\mathbb{P}(|X_n - x^*| > \mathbf{c}_1 n^{-\alpha/d}) \leq \mathbf{c}_2 n^{\alpha-\alpha_2} \leq \delta,$$

which illustrates the rate of algebraic convergence. \square

Let us conclude this section with the following remark. Our focus here is on the challenge of proving convergence of the sequence $\{X_n\}_{n \geq 0}$ generated by the algorithm (1.2). In the literature, very often, the easier problem of convergence for the sequence

$$(3.47) \quad \tilde{X}_n := \min\{X_0, \dots, X_n\}$$

is studied. For such a sequence, we can derive the following stronger result for the algorithm under the conditions of Theorem 2.1.

COROLLARY 3.11. *Under the same assumptions as in Theorem 2.1, the sequence $\{\tilde{X}_n\}_{n \geq 0}$ defined in (3.47) converges almost surely to x^* .*

Proof. This is a direct consequence of the fact that $\{\tilde{X}_n\}_{n \geq 0}$ is monotone decreasing and bounded from below by x^* . It thus has a limit, say, X^- . By Property One of Subsection 3.1, X^- is equal to x^* with probability 1. \square

4. Parameter Estimations and Algorithmic Details. The main contribution of this paper is to show that it is possible to achieve an algebraic rate of convergence in probability and location by using an SGD algorithm with a state-dependent variance when finding the global minimizer of

a nonconvex optimization problem. We have presented the proposed algorithm (2.1) and rigorously proved the convergence of the algorithm in Section 3. The proof is valid under quite general conditions on the objective function, which is further supported by the numerical results later in Subsection 5.1.

For an explicit implementation of the proposed SGD algorithm, we also need to obtain the two essential components that directly define the proposed SGD algorithm in (1.5): the state-dependent variance function $\sigma_n(f(x))$ and the step size η_n . In particular, the state-dependent variance in (2.1) is directly determined by two scalar variables that change with the iteration number n : f_n (the cutoff value that determines the sublevel-set Ω_n), σ_n (the decaying variance inside Ω_n).

There are many types of heuristic strategies to set η_n , f_n and σ_n , such as parameter tuning, which is common in implementing practical algorithms for complex optimization problems. Some of the strategies are presented in the numerical examples (see Subsection 5.1). In this section, we discuss a few particular approaches to set these scalars.

4.1. Given Estimates of $\Omega^*(f)$, b_1 and b_2 . First, assume that we have already obtained good estimates for the function $\Omega^* : \mathbb{R} \mapsto \mathbb{R}^+$,

$$(4.1) \quad \Omega^*(f) = |\{x \in \mathfrak{X} | f(x) \leq f\}|,$$

which maps the cutoff objective function value f to the volume of the f -sublevel set of the objective function $f(x)$. Note that $\Omega^*(f)$ is a monotonically increasing function of f . Mathematically, we are given two monotonically increasing functions $\underline{\Omega}(f)$ and $\overline{\Omega}(f)$ such that $\forall f$,

$$\underline{\Omega}(f) \leq \underline{\gamma}\Omega^*(f) \leq \Omega^*(f) \leq \overline{\gamma}\Omega^*(f) \leq \overline{\Omega}(f),$$

where $0 < \underline{\gamma} \leq 1 \leq \overline{\gamma} < \infty$. Moreover, we assume to have the upper and lower bounds for b_1 and b_2 ; see A1 for their definitions. That is, we are given two estimated scalars \underline{b}_1 and \overline{b}_2 such that

$$0 < \underline{b}_1 \leq b_1 \leq b_2 \leq \overline{b}_2 < \infty.$$

Recall that Assumption B3 requires a pre-determined decay rate for the volume of the f_n -sublevel set, i.e., $|\Omega_n|$, in terms of the iteration number n . Our main result Theorem 2.1 and its proof in Section 3 are based upon this assumption. Utilizing the estimations of function $\Omega^*(f)$, we could set the sequence $\{f_n\}$ for each n by choosing the inverse of function $\overline{\Omega}(f)$ evaluated at the sequence $\{|\Omega_n|\}$ based on the pre-determined decay rate in B3 using estimations \underline{b}_1 and \overline{b}_2 . Since $\overline{\Omega}(f)$ is monotonically increasing, its general inverse function is well-defined, and the estimated $\{f_n\}$ will be monotonically decreasing with respect to n . The value can be practically computed through numerical interpolation. Once we have the pre-determined values for $\{|\Omega_n|\}$, the variable σ_n can be set accordingly in order to satisfy Assumption B2. Based on Assumption B1, we may choose the step size as a constant $\eta_n = \eta < 2/\overline{b}_2$. As a result, all three essential assumptions B1-B3 are satisfied, for which Theorem 2.1 will follow.

4.2. Estimations of $\Omega^*(f)$, \underline{b}_1 and \overline{b}_2 . In Subsection 4.1, we rely on good estimations of $\Omega^*(f)$, \underline{b}_1 and \overline{b}_2 . Here, we discuss several ways to obtain estimations of the required quantities that were assumed to be known earlier.

4.2.1. Monte Carlo Estimation of $\Omega^*(f)$. Recall that the sublevel set Ω_n is associated with the small variance σ_n . Since the noise power of the proposed SGD algorithm (2.1) inside the low-variance subset, characterized by σ_n , depends on the Lebesgue measure of the sublevel set Ω_n , which is implicitly controlled by the cutoff value f_n , it is thus important to estimate the relation between f_n and $|\Omega_n|$. That is, the function $\Omega^*(f)$ defined in (4.1), if not known a priori.

Let $f_{max} = \max_{x \in \mathfrak{X}} f(x)$. Given any scalar $f \in [f^*, f_{max}]$, we define

$$(4.2) \quad \mathcal{G}(f) := \frac{\Omega^*(f)}{|\mathfrak{X}|} = \int_{\mathfrak{X}} \mathbb{1}_{f(x) \leq f} p(x) dx = \int_{\mathfrak{X}} \mathfrak{I}_f(x) p(x) dx, \quad \mathfrak{I}_f(x) := \mathbb{1}_{f(x) \leq f},$$

where the probability density function $p(x) = 1/|\mathfrak{X}|$, denoting the uniform distribution over the domain \mathfrak{X} . We may estimate $\mathcal{G}(\mathfrak{f})$ by a Monte Carlo quadrature denoted as $\mathcal{F}_N(\mathfrak{f})$ where

$$(4.3) \quad \mathcal{F}_N(\mathfrak{f}) = \frac{1}{N} \sum_{i=1}^N \mathbb{1}_{f(Y_i) \leq \mathfrak{f}} = \frac{1}{N} \sum_{i=1}^N \mathcal{I}_{\mathfrak{f}}(Y_i).$$

Here, $\{Y_i\}$ are N i.i.d. samples following $p(x)$, i.e., uniform samples from the domain \mathfrak{X} . So far, we have two cumulative distribution functions \mathcal{F}_N and \mathcal{G} where \mathcal{F}_N is regarded as a Monte Carlo estimation of \mathcal{G} . Based on classic theories of the Monte Carlo methods [2],

$$(4.4) \quad \mathcal{F}_N(\mathfrak{f}) \approx \mathcal{G}(\mathfrak{f}) + \frac{\sigma(\mathcal{I}_{\mathfrak{f}})}{\sqrt{N}} \nu_1, \quad \forall \mathfrak{f} \in [\mathfrak{f}^*, \mathfrak{f}_{max}],$$

where $\nu_1 \sim \mathcal{N}(0, 1)$ and the standard deviation $\sigma(\mathcal{I}_{\mathfrak{f}})$ satisfies

$$(4.5) \quad \sigma(\mathcal{I}_{\mathfrak{f}})^2 = \int_{\mathfrak{X}} \mathcal{I}_{\mathfrak{f}}^2 p(x) dx - \mathcal{G}(\mathfrak{f})^2 = \mathcal{G}(\mathfrak{f}) - \mathcal{G}(\mathfrak{f})^2 \leq \frac{1}{4}.$$

For our proposed SGD algorithm (2.1), we need a sequence of cutoff function values $\{f_n\}$ such that $\mathcal{G}(f_n) = n^{-\alpha}$ for a given $\alpha > 0$, as required by Assumption B3. Based on the estimated function \mathcal{F}_N , we obtain a sequence of estimation $\{\hat{f}_{n,N}\}$ such that

$$(4.6) \quad \mathcal{F}_N(\hat{f}_{n,N}) = \mathcal{G}(f_n) = n^{-\alpha}.$$

Next, we will prove that the estimated cutoff value $\hat{f}_{n,N}$ will converge in probability to the true f_n as the number of samples $N \rightarrow \infty$.

We start with the following assumptions.

D1 There exists $\tilde{\mathfrak{f}}$ such that $\{x : f(x) \leq \tilde{\mathfrak{f}}\} \subseteq \Omega_{sc}$ and the objective function $f(x) \in C^3(\Omega_{sc})$ is locally quadratic.

D2 For any $\mathfrak{f} \in (\tilde{\mathfrak{f}}, \mathfrak{f}_{max})$, there exists a constant \underline{L} such that $\inf_{\delta > 0} \frac{\mathcal{G}(\mathfrak{f}+\delta) - \mathcal{G}(\mathfrak{f})}{\delta} > \underline{L} > 0$.

THEOREM 4.1. *Let A1, A2, B3, D1 and D2 hold. Consider $\hat{f}_{n,N}$ defined in (4.6) with $N \geq n$, and a given $\alpha \in (0, 1)$. Then for all $\epsilon > 0$,*

$$(4.7) \quad \lim_{N \rightarrow \infty} \mathbb{P}(|\hat{f}_{n,N} - f_n| < \epsilon) = 1.$$

Proof. Based on Assumption D2, for any two $\mathfrak{f}_1, \mathfrak{f}_2 \in (\tilde{\mathfrak{f}}, \mathfrak{f}_{max})$, we have

$$(4.8) \quad \begin{aligned} |\mathcal{F}_N(\mathfrak{f}_1) - \mathcal{F}_N(\mathfrak{f}_2)| &= |\mathcal{F}_N(\mathfrak{f}_1) - \mathcal{G}(\mathfrak{f}_1) + \mathcal{G}(\mathfrak{f}_1) - \mathcal{G}(\mathfrak{f}_2) + \mathcal{G}(\mathfrak{f}_2) - \mathcal{F}_N(\mathfrak{f}_2)| \\ &> \underline{L}|\mathfrak{f}_1 - \mathfrak{f}_2| - |\mathcal{F}_N(\mathfrak{f}_1) - \mathcal{G}(\mathfrak{f}_1)| - |\mathcal{F}_N(\mathfrak{f}_2) - \mathcal{G}(\mathfrak{f}_2)|. \end{aligned}$$

Furthermore, there exists $\mathfrak{n} \in \mathbb{N}$ such that $f_{\mathfrak{n}+1} \leq \tilde{\mathfrak{f}} < f_{\mathfrak{n}}$ where $\{f_n\}$ are defined by (4.6). Clearly, $\tilde{\mathfrak{f}} < f_n$ for any $n \leq \mathfrak{n}$. With \mathfrak{f}_1 replaced by $\hat{f}_{n,N}$, and \mathfrak{f}_2 replaced by f_n , (4.8) yields

$$\begin{aligned} |\hat{f}_{n,N} - f_n| &\leq \frac{1}{\underline{L}} \left(|\mathcal{F}_N(\hat{f}_{n,N}) - \mathcal{F}_N(f_n)| + |\mathcal{G}(f_n) - \mathcal{F}_N(f_n)| + |\mathcal{G}(\hat{f}_{n,N}) - \mathcal{F}_N(\hat{f}_{n,N})| \right) \\ &= \frac{1}{\underline{L}} \left(2|\mathcal{G}(f_n) - \mathcal{F}_N(f_n)| + |\mathcal{G}(\hat{f}_{n,N}) - \mathcal{F}_N(\hat{f}_{n,N})| \right). \end{aligned}$$

As a result, for any $\epsilon > 0$, we have the following by Chebyshev's inequality and (4.5).

$$(4.9) \quad \begin{aligned} &\mathbb{P}(|\hat{f}_{n,N} - f_n| < \epsilon) \\ &\geq \mathbb{P}(\{|\mathcal{G}(f_n) - \mathcal{F}_N(f_n)| < \epsilon/(3\underline{L})\} \cap \{|\mathcal{G}(\hat{f}_{n,N}) - \mathcal{F}_N(\hat{f}_{n,N})| < \epsilon/(3\underline{L})\}) \\ &\geq 1 - \mathbb{P}(|\mathcal{G}(f_n) - \mathcal{F}_N(f_n)| \geq \epsilon/(3\underline{L})) - \mathbb{P}(|\mathcal{G}(\hat{f}_{n,N}) - \mathcal{F}_N(\hat{f}_{n,N})| \geq \epsilon/(3\underline{L})) \geq 1 - \frac{9\underline{L}^2}{2N\epsilon^2}. \end{aligned}$$

When $n > \mathfrak{n}$, we have $f_n \leq \tilde{\mathfrak{f}}$ and thus $\Omega_n \subseteq \{x : f(x) \leq \tilde{\mathfrak{f}}\} \subseteq \Omega_{sc}$ by **D1**. We also have that $f(x) \in C^3(\Omega_{sc})$ according to **D1**, and

$$(4.10) \quad f(x) = f^* + (x - x^*)^\top H(x - x^*) + o(|x - x^*|^2), \quad \forall x \in \Omega_{sc},$$

where $H = \nabla^2 f(x^*)$ is positive definite. Thus, $\mathcal{G}(\mathfrak{f})$ is continuously differentiable for $\mathfrak{f} \leq \tilde{\mathfrak{f}}$. According to (3.22) and (4.6), $n^{-\alpha} = \mathcal{G}(f_n) = \mathcal{O}((f_n - \mathfrak{f}^*)^{d/2})$, which leads to $f_n - \mathfrak{f}^* = \mathcal{O}(n^{-2\alpha/d})$. Consequently, $\mathcal{G}'(f_n) = \mathcal{O}((f_n - \mathfrak{f}^*)^{d/2-1}) = \mathcal{O}(n^{-\alpha(1-2/d)})$. We remark here that as $n \rightarrow \infty$, $\mathcal{G}'(f_n) \rightarrow \infty$ for $d = 1$, remains constant for $d = 2$, and goes to zero for $d \geq 3$. Here, analyzing the error $|\hat{f}_{n,N} - f_n|$ links to the sensitivity analysis for the root-finding problem [7, Chapter 3]. We apply the classical result and obtain

$$(4.11) \quad |\hat{f}_{n,N} - f_n| \approx \left| \frac{\mathcal{G}(f_n) - \mathcal{F}_N(f_n)}{\mathcal{G}'(f_n)} \right|.$$

Finally, for any $\epsilon > 0$, by Chebyshev's inequality and (4.5), we have

$$(4.12) \quad \mathbb{P}(|\hat{f}_{n,N} - f_n| \geq \epsilon) \approx \mathbb{P}(|\mathcal{G}(f_n) - \mathcal{F}_N(f_n)| \geq \mathcal{G}'(f_n)\epsilon) \leq \frac{n^{2\alpha(1-\frac{2}{d})}}{CN\epsilon^2},$$

where $C > 0$ is a constant. When $d \leq 2$, the numerator of the last term monotonically decreases, so $\mathbb{P}(|\hat{f}_{n,N} - f_n| \geq \epsilon)$ decreases at least with the rate $\mathcal{O}(N^{-1})$. When $d > 2$, we have $\alpha < \frac{1}{2}$ by Assumption **B3**, and thus $2\alpha(1 - \frac{2}{d}) < 1$. We also have $\mathbb{P}(|\hat{f}_{n,N} - f_n| \geq \epsilon)$ decreases as $N \rightarrow \infty$ since $n \leq N$ by assumption.

The proof is complete by combining (4.9) and (4.12). \square

Remark 4.2. Equation (4.5) shows that the absolute error in the Monte Carlo estimation is small when $\Omega^*(\mathfrak{f}) \rightarrow 0$ (or equivalently when $\mathfrak{f} \rightarrow \mathfrak{f}^*$) as well as when $\Omega^*(\mathfrak{f}) \rightarrow |\mathfrak{X}|$ (or equivalently when $\mathfrak{f} \rightarrow \mathfrak{f}_{max}$). On the other hand, the error is the largest when $\Omega^*(\mathfrak{f}) = |\mathfrak{X}|/2$. This observation matches the numerical results shown in Figure 9c.

Although the proof in Section 2 is based on the setup (2.1), it is sometimes more convenient to draw a sample with high-variance variance σ_n^+ rather than a uniform sample from \mathfrak{X} when $X_n \in \Omega_n^c$. In that case, the Monte Carlo estimation described above requires many additional objective function evaluations, which could be computationally prohibitive for large-scale problems. An alternative approach is to utilize the iterates $\{X_n\}$ that are already generated as we execute the proposed SGD algorithm (1.5). This is what we refer to as the online estimation. However, based on (1.5), the iterates $\{X_n\}$ are neither independent nor following the uniform distribution. Nevertheless, one could still *estimate* the relation between \mathfrak{f} and $\Omega^*(\mathfrak{f})$ using the high-variance iterates. Here, we say X_{n+1} is a high-variance iterate if $X_n \in \Omega_n^c$ and thus $\mathbb{P}(X_{n+1}|X_n)$ is subject to the large noise coefficient σ_n^+ in (1.6). The larger the noise coefficient σ_n^+ is, the less the iterate X_{n+1} is correlated with X_n , which makes X_{n+1} closer to being a uniform sample drawn from the domain \mathfrak{X} . Later in Subsection 5.3, we will present a numerical example to demonstrate the effectiveness of such online estimation of $\Omega^*(\mathfrak{f})$ by using the high-variance iterates compared with the estimation using the i.i.d. uniform samples.

4.2.2. Estimating b_1 and b_2 . Note that b_1 and b_2 are lower and upper bounds for the eigenvalues of $\nabla^2 f(x)$, $x \in \Omega_{sc}$. Since $f(x)$ is locally quadratic in Ω_{sc} based on (4.10), we may regard the smallest and the largest eigenvalues of $H = \nabla^2 f(x^*)$ as b_1 and b_2 , respectively.

Given any set of scalar values $\{g_n\}$ where $g_n \xrightarrow{n \rightarrow \infty} \mathfrak{f}^*$, for n large enough, we have

$$\Pi_n := \{x : f(x) \leq g_n\} \subseteq B_{\Pi_n} := \{x : |x - x^*| \leq \sqrt{2(g_n - \mathfrak{f}^*)/\lambda_1}\},$$

where $0 < \lambda_1 \leq \dots \leq \lambda_d < \infty$ are eigenvalues of H . The diameter of B_{Π_n} is $2\sqrt{2(g_n - \mathfrak{f}^*)/\lambda_1}$, which could be approximated by $\text{diam}(\Pi_n)$. Recall that $\text{diam}(A) = \sup_{y_1, y_2 \in A} |y_1 - y_2|$. Thus,

$$(4.13) \quad b_1 \approx \lambda_1 = \lim_{n \rightarrow \infty} \frac{8(g_n - \mathfrak{f}^*)}{|\text{diam}(B_{\Pi_n})|^2} \approx \lim_{n \rightarrow \infty} \frac{8(g_n - \mathfrak{f}^*)}{\sup_{f(y_1), f(y_2) \leq g_n} |y_1 - y_2|^2}.$$

On the other hand, we may approximate the largest eigenvalue λ_d by the maximum slope of the gradient function $G(x)$ at $x = x^*$. That is,

$$(4.14) \quad b_2 \approx \lambda_d = \sup_{y \neq 0} \frac{y^\top Hy}{y^\top y} = \lim_{n \rightarrow \infty} \sup_{f(y_1), f(y_2) \leq g_n} \frac{|G(y_1) - G(y_2)|}{|y_1 - y_2|}.$$

Note that estimations based on (4.13) and (4.14) are only valid once we have access to samples from Ω_{sc} . On the other hand, the accuracy of b_1 and b_2 estimations only become relevant to the convergence rate of the SGD algorithm once $\Omega_n \subseteq \Omega_{sc}$. Taking both aspects into account, we propose the following iterative algorithm to approximate b_1 and b_2 .

Consider i.i.d. samples $\{Y_n\}$ drawn uniformly from the domain \mathfrak{X} , and the set of scalar values $\{g_n\}$ where $g_n \rightarrow \mathfrak{f}^*$. For a given $m \in \mathbb{N}$, we first select m samples where

$$\{y_{n_1}, y_{n_2}, \dots, y_{n_m}\} \subseteq \{y_1, y_2, \dots, y_{n_m}\}$$

such that $f(Y_{n_i}) \leq g_1$ for $i = 1, \dots, m$. Using those m samples, we estimate b_1 and b_2 based on (4.13) and (4.14). For $k = 1, \dots, m - 1$,

$$\begin{aligned} \hat{b}_2^{(1)} &\leftarrow \max \left(\hat{b}_2^{(1)}, \frac{|G(Y_{n_{k+1}}) - G(Y_{n_k})|}{|Y_{n_{k+1}} - Y_{n_k}|} \right), \\ \hat{\mathfrak{f}}^* &\leftarrow \min (\hat{\mathfrak{f}}^*, f(Y_{n_k})), \\ \hat{D}^{(1)} &\leftarrow \max (\hat{D}^{(1)}, |Y_{n_{k+1}} - Y_{n_k}|), \end{aligned}$$

and finally, with the best $\hat{\mathfrak{f}}^*$ and $\hat{D}^{(1)}$ estimated from the m samples, we set

$$\hat{b}_1^{(1)} = 8|g_1 - \hat{\mathfrak{f}}^*|/\hat{D}^{(1)}.$$

We may then use $\hat{b}_1^{(1)}$ and $\hat{b}_2^{(1)}$ to obtain $\alpha^{(1)}$ as an estimator for the true α based on B3, followed by estimations of f_n as discussed in Subsection 4.2.1.

Since we do not know where the set Ω_{sc} is a priori, the estimation process has to be repeated to obtain accurate approximations of b_1 and b_2 . We summarize the algorithm in Algorithm 4.1.

Algorithm 4.1 Estimation of b_1 and b_2

- 1: Given i.i.d. uniform samples $\{Y_n\}$, $m \in \mathbb{N}$, and scalar values $\{g_n\}$ where $g_n \rightarrow \mathfrak{f}^*$. Set $\hat{\mathfrak{f}}^* = f(Y_1)$.
 - 2: **for** $l = 1, 2, \dots$ **do**
 - 3: Set $k_l = ml(l-1)/2$ and $\hat{b}_2^{(l)} = \hat{D}^{(l)} = i = 0$.
 - 4: **while** $i < ml$ **do**
 - 5: **if** $f(Y_n) < g_{1+k_l}$ **then**
 - 6: Update $i \leftarrow i + 1$, and set $Y_{n_s} = Y_n$ where $s = i + k_l$.
 - 7: Update $\hat{\mathfrak{f}}^* \leftarrow \min (\hat{\mathfrak{f}}^*, f(Y_{n_s}))$.
 - 8: **if** $i \geq 2$ **then**
 - 9: Update $\hat{D}^{(l)} \leftarrow \max (\hat{D}^{(l)}, |Y_{n_s} - Y_{n_{s-1}}|)$, and $\hat{b}_2^{(l)} \leftarrow \max \left(\hat{b}_2^{(l)}, \frac{|G(Y_{n_s}) - G(Y_{n_{s-1}})|}{|Y_{n_s} - Y_{n_{s-1}}|} \right)$.
 - 10: **end if**
 - 11: **end if**
 - 12: **end while**
 - 13: Set $\hat{b}_1^{(l)} = 8|g_{1+k_l} - \hat{\mathfrak{f}}^*|/\hat{D}^{(l)}$. Obtain $\alpha^{(l)}$ based on $\hat{b}_1^{(l)}$ and $\hat{b}_2^{(l)}$.
 - 14: Estimate $\{f_n\}$ for $n = 1 + k_l, 2 + k_l, \dots, k_{l+1}$.
 - 15: **end for**
-

4.2.3. Estimating \underline{b}_1 and \overline{b}_2 . While [Subsection 4.2.2](#) discusses how to approximate b_1 and b_2 accurately by repeating the process with selected uniform samples that are gradually more likely to be drawn from Ω_{sc} , we present here an algorithm that provides crude lower and upper bounds for b_1 and b_2 , respectively. We remark that although this algorithm is more straightforward, it will result in a slower algebraic convergence rate due to the possible severe under- and over-estimations.

Based on [\(4.13\)](#), an upper bound for b_2 , denoted as \overline{b}_2 , can be obtained based on the divided difference. Given two consecutive iterates X_n and X_{n+1} , we compute

$$(4.15) \quad E_n = \frac{|G(X_{n+1}) - G(X_n)|}{|X_{n+1} - X_n|},$$

which gives us a sequence of estimates $\{E_n\}$. Within the sequence, we treat the largest value as an upper bound for b_2 , denoted as \overline{b}_2 .

Using similar arguments in [Lemma 3.6](#), for sufficiently large n , we have $\Pi_n \subseteq \Omega_{sc}$ and Π_n is nested between two ellipsoids centered at x^* whose quadratic forms are defined by $\nabla^2 f(x^*)$. We also have

$$(4.16) \quad \lim_{n \rightarrow \infty} |\Pi_n|^{-2} (2(g_n - f^*)/c_0^2)^d = \det(\nabla^2 f(x^*)) = \lambda_1 \dots \lambda_d \leq \lambda_1 \lambda_d^{d-1}.$$

Since $\lambda_d \leq b_2 \leq \overline{b}_2$, we may use \mathcal{E}_n as a lower bound estimation for λ_1 where

$$(4.17) \quad \lambda_1 \geq \mathcal{E}_n = (\overline{b}_2)^{1-d} |\Pi_n|^{-2} (2(g_n - f^*)/c_0^2)^d.$$

Among the sequence $\{\mathcal{E}_n\}$, we select the smallest value as a lower-bound estimate for b_1 . We remark that in practice, if f^* is known, then we always have that $g_n > f^*$ by construction. If f^* is unknown and needs to be estimated, one should use the minimum value in any finite sequence $\{g_n\}$. We also have $g_n > f^*$ until the last element of the finite sequence, when the estimation [\(4.17\)](#) should stop. We also comment that if the function $f(x)$ satisfies our assumption, the ratio $(g_n - f^*)^d / |\Pi_n|^2$ should be non-vanishing although both sides of the fraction go to zero as n increases. For any given g_n , estimating the volume of Π_n can be achieved by the Monte Carlo method; see [Subsection 4.2.1](#) for details.

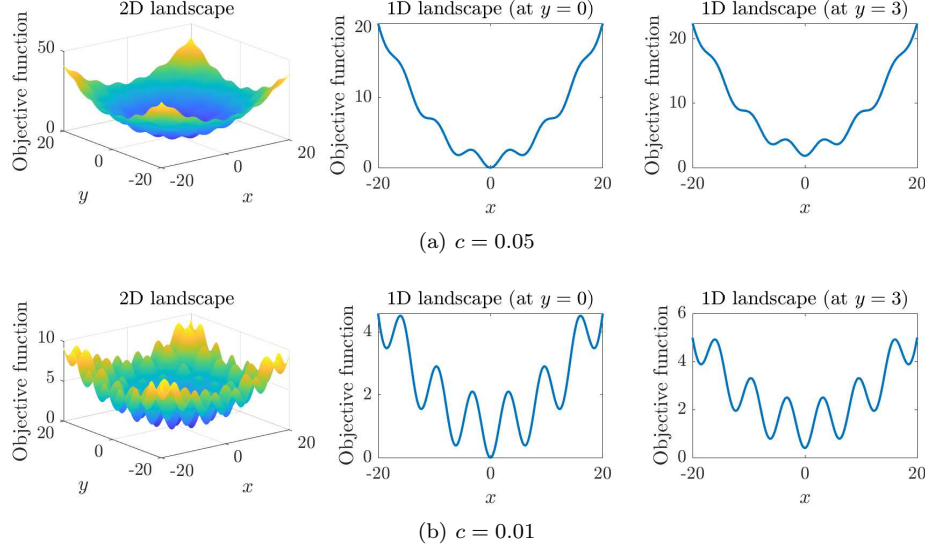
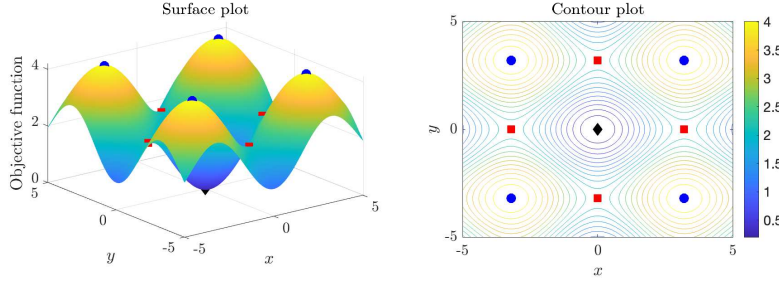
We summarize the scheme of obtaining a lower bound \underline{b}_1 and an upper bound \overline{b}_2 into [Algorithm 4.2](#).

Algorithm 4.2 Estimation of \underline{b}_1 and \overline{b}_2

- 1: Given the initial iterate X_0 , compute X_1 based on [\(2.1\)](#). Set $\underline{b}_1 = \overline{b}_2 = \frac{|G(X_0) - G(X_1)|}{|X_0 - X_1|}$.
 - 2: **for** $n = 2$ to n_{tot} **do**
 - 3: Obtain g_n , (estimations of) $|\Pi_n|$ and f^* . Given X_{n-1} , compute X_n based on [\(2.1\)](#).
 - 4: Update $\overline{b}_2 \leftarrow \max\left(\overline{b}_2, \frac{|G(X_n) - G(X_{n-1})|}{|X_n - X_{n-1}|}\right)$ and $\underline{b}_1 \leftarrow \min(\underline{b}_1, \mathcal{E}_n)$ where \mathcal{E}_n follows [\(4.17\)](#).
 - 5: **end for**
-

5. Numerical Examples. We have given analysis in the previous sections regarding the convergence of the proposed AdaVar algorithm [\(2.1\)](#). In [Subsection 5.1](#) below, we present a few simple numerical examples to quantitatively demonstrate the effectiveness of the proposed algorithm. The use of an adaptive state-dependent variance is very powerful, and we give two examples in [Subsection 5.2](#) where this technique is applied to settings that are not theoretically discussed in this paper. We will also discuss such settings in [Section 6](#) under future directions. In [Subsection 5.3](#), we provide an example corresponding to the estimations discussed in [Section 4](#).

5.1. The AdaVar Algorithm [\(2.1\)](#) Applied to Global Optimization Problems. In this subsection, we present a numerical optimization example to show the quantitative convergence of our proposed algorithm for finding the global minimizer of a highly nonconvex function. In the following set of tests, we consider a variation of the so-called Rastrigin function [\[19\]](#) as our objective function

Fig. 2: Optimization landscape of J_1 for $a = b = 1$, $c = 0.05, 0.01$.Fig. 3: The zoom-in illustration of J_1 for $a = b = 1, c = 0.01$ on the domain $[-5, 5]^2$. The red squares represent the saddle points, the blue circles highlight the local minima and the black diamond marks the global minimizer.

$J_1(\mathbf{x})$ where $\mathbf{x} = (x_1, x_2, \dots, x_d)^\top \in \mathbb{R}^d$.

$$(5.1) \quad J_1(\mathbf{x}) = a \left(d - \sum_{i=1}^d \cos(bx_i) \right) + c \sum_{i=1}^d x_i^2.$$

When $c = 0$, all local minima of J_1 are global minima. When $c > 0$, J_1 has a unique global minimizer $x^* = (0, 0)$ and infinitely many local minima and saddle points in \mathbb{R}^d . In terms of numerical implementation, we truncate our search domain Ω to be $[-20, 20]^d$.

5.1.1. Two-Dimensional Objective Function. First, we consider $d = 2$. Fixing $a = b = 1$, we focus on two cases: $c = 0.05$ and $c = 0.01$. The search domain $\Omega = [-20, 20]^2$; see Figure 2 for illustrations of the optimization landscapes. In Figure 3, we highlight the global minimizer together with local minima and saddle points in the subset $[-5, 5]^2$ for $c = 0.01$.

We use the proposed SGD algorithm to minimize J_1 , which mainly follows (2.1). In terms of practical implementation, hyperparameters of the proposed algorithm could be treated as tunable parameters, like in many other optimization algorithms. Here, we set $\eta = 1$, $\sigma_0 = 1$ and $\tilde{\sigma}_0 = 20$. We

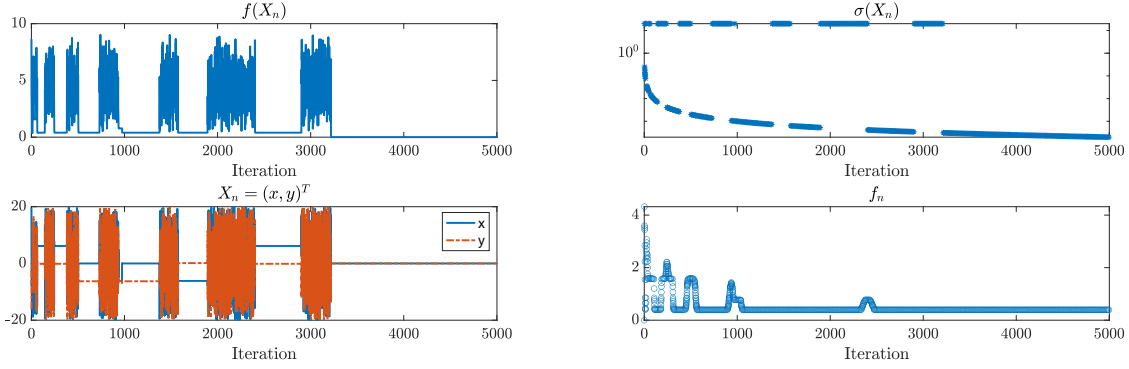


Fig. 4: Convergence history of minimizing J_1 for $c = 0.01$ with the state-dependent noise following (5.2): the objective function value (top left), the standard deviation of the iterate (top right), the location of the iterates (bottom left), and the cutoff value that decides the sublevel set, i.e., the low-variance region (bottom right).

remark that the most important elements of the proposed algorithm are the state-dependent standard deviation $\sigma_n(f(x))$ of the noise term and the cutoff value f_n . We set

$$(5.2) \quad \sigma_n(f(x)) = \begin{cases} \sigma_0 n^{-\alpha}, & f(x) < f_n, \\ \tilde{\sigma}_0, & f(x) \geq f_n, \end{cases}$$

where the cutoff value f_n is the median (0.5 quantile) of the objective function values from the first n iterations, $\{J_1(X_0), J_1(X_1), \dots, J_1(X_n)\}$. In this 2D example, we choose $\alpha = 1$. Without further information about $J(x)$, one could treat α as a tunable parameter. Due to the state-dependent bias imposed by (5.2), $\{X_n\}$ are more likely to stay at regions with small objective function values.

We present the convergence history of a single run of the algorithm in Figure 4 for the case $c = 0.01$. In Figure 5, we summarize the estimated probability of convergence with respect to the number of iterations and compare between the classical method (1.4) where $\sigma_n = 1/\sqrt{n}$ and our proposed method (1.5) where σ_n is defined through (5.2). One can observe that the iterate X_n converges to the global minimum x^* in probability for both $c = 0.01$ and $c = 0.05$ using our proposed method, while with the classical method, there is no visible convergence. Quantitatively, using our proposed method, $\mathbb{P}(|X_n - x^*| < 0.01) \approx 1.000$ for $c = 0.05$ and $\mathbb{P}(|X_n - x^*| < 0.01) \approx 0.997$ for $c = 0.01$, while for the classical method, $\mathbb{P}(|X_n - x^*| < 0.01) \leq 1\%$ for both cases after 5×10^3 iterations. The statistics are estimated by 10^3 independent runs with the starting point X_0 uniformly sampled from the domain Ω .

It takes more iterations for the case $c = 0.01$ than the case $c = 0.05$ as there are more local minima and saddle points within the domain Ω as c decreases. Besides, the difference in the objective function value between the global minimum and the closest local minimum becomes smaller. Also, the difference in objective function value between the neighboring local minimum and maximum is much larger. The latter difference is often referred to as the energy barrier, commonly used in the context of phase transition and chemical reactions [10]. Using our algorithm to induce phase transition in chemistry, thermodynamics, and other related fields could be one potential application of interest [9].

5.1.2. Ten-Dimensional Objective Function. Next, we consider minimizing J_1 defined in (5.1) for the case $d = 10$. The number of local minima and saddle points in the search domain $\Omega = [-20, 20]^d$ has increased exponentially in terms of d , demonstrating the curse of dimensionality in large-scale non-convex optimization problems. We address that the basin of attraction is extremely small as it is approximately 10^{-10} of the entire search domain. In this 10D example, we consider $c = 0.03$ and $c = 0.05$ while fixing $a = b = 1$ as before. Similar to the 2D case, we set $\eta = 1$, $\sigma_0 = 1$, and $\tilde{\sigma}_0 = 20$. There is a slight difference in the setting of σ_n due to a more complex optimization landscape for

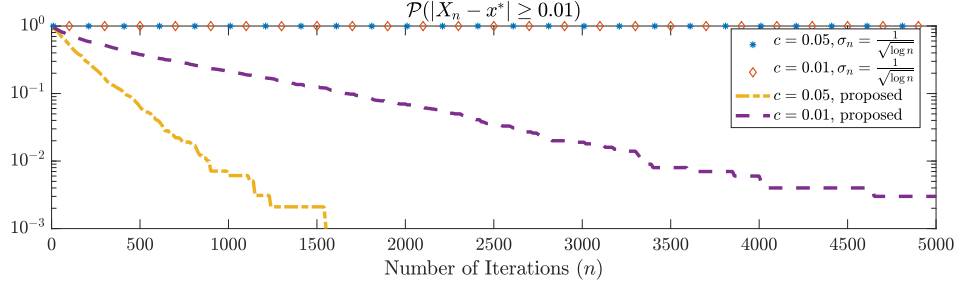


Fig. 5: 2D global optimization: estimation of $\mathbb{P}(|X_n - x^*| \geq 0.01)$ using 10^3 independent runs where X_n follows the classical method (1.4) and the proposed SGD algorithm (1.5) with variance defined in (5.2), respectively. The objective function is J_1 defined in (5.1) with $d = 2$ and $c = 0.05$ or $c = 0.01$.

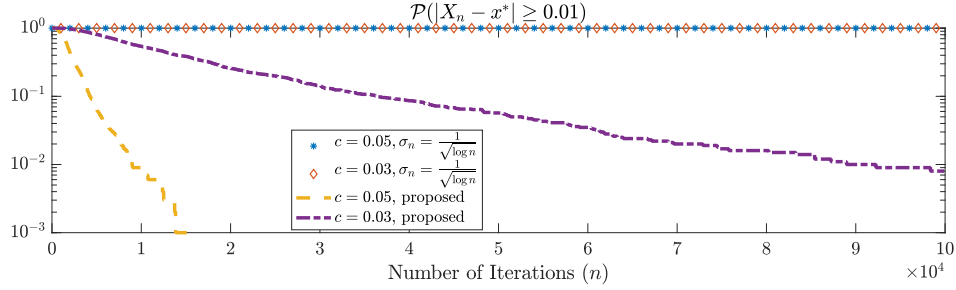


Fig. 6: 10D global optimization: estimation of $\mathbb{P}(|X_n - x^*| \geq 0.01)$ using 10^3 independent runs where X_n follows the classical method (1.4) and the proposed SGD algorithm (1.5) with variance defined in (5.2), respectively. The objective function is J_1 defined in (5.1) with $d = 10$ and $c = 0.05$ or $c = 0.03$.

$d = 10$: we choose $\alpha = 0.5$ in (5.2) instead of $\alpha = 1$ in the 2D case. The slower decay in σ_n is to ensure that the iterates can visit the global basin of attraction before the variance becomes extremely small such that it becomes harder for the iterates to escape a local minimum. It also illustrates the flexibility by considering α as a tunable parameter in practical implementations. The cutoff value f_n is still the median (0.5-quantile) of the set $\{J_1(X_0), J_1(X_1), \dots, J_1(X_n)\}$.

The convergence histories of different setups using both the proposed method and the classical method are shown in Figure 6. One can observe the noticeably faster convergence of the proposed method as a result of the state-dependent variance. Compared to the 2D case, the 10D case requires more iterations to satisfy $\mathbb{P}(|X_n - x^*| < 0.01)$ due to the more complicated optimization landscapes of J_1 in higher dimensions. One can still observe the almost exponential convergence. Quantitatively, using our proposed method, $\mathbb{P}(|X_n - x^*| < 0.01) \approx 1.000$ for $c = 0.05$ and $\mathbb{P}(|X_n - x^*| < 0.01) \approx 0.992$ for $c = 0.03$, while for the classical method, $\mathbb{P}(|X_n - x^*| < 0.01) \approx 0$ in both cases within 10^5 iterations. Again, the statistics are estimated by 10^3 independent runs with uniformly sampled starting points. If we use uniform sampling to find an initial guess in the global basin of attraction, we may need approximately $(\frac{7}{40})^{-10} \approx 3.7 \times 10^7$ different samples for the case $c = 0.05$ in which the global basin of attraction is a subset of the hyper-cube $[-3.5, 3.5]^{10}$, while our domain is $[-20, 20]^{10}$.

5.2. State-Dependent Variance Techniques Applied to Other Stochastic Descent Problems. This subsection presents two numerical examples based on more general settings than the one discussed earlier in this paper. One deals with stochastic objective functions as mentioned on the connection to formula (1.3)—the other concerns gradient-free optimization. The promising numerical results demonstrate the power of adaptive state-dependent variance and indicate the potential for

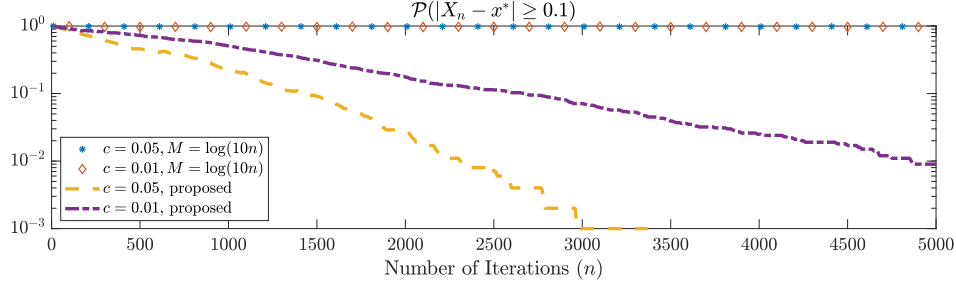


Fig. 7: 2D global optimization where the loss function is estimated by sampling (see Subsection 5.2.1): the semi-log plots of $\mathbb{P}(|X_n - x^*| \geq 0.1)$ using the classical method (1.4) (batch size version) and the proposed algorithm (5.5) with a state-dependent batch size to optimize J_2 defined in (5.4) where $a = b = 1$, $d = 2$, $c = 0.01$ and $c = 0.05$.

generalizing this work.

5.2.1. Sampling of the Objective Function. One very important application of stochastic gradient descent is machine learning. The random component is then not decoupled from the objective or loss function. Although this was not the setting proved in Section 3, we present a simple numerical example below showing the favorable outcomes in the case of sampling.

As we have introduced in Section 1, the stochastic gradient descent method used in machine learning applications often has the form of (1.3) where the variance is encoded in the estimated gradient $G(X_n; \xi)$ and ξ is a random variable. For example, we are interested in finding the global minimum of the following optimization problem

$$(5.3) \quad \min_x \mathbb{E}_\zeta[J(x; \zeta)] \approx \frac{1}{M} \sum_{i=1}^M J(x; \zeta_i) = \tilde{J}(x),$$

where M is the size of the training set (or sampled data) and $\{\zeta_i\}$ are i.i.d. samples following the distribution of ζ . For each i , the gradient $G(x; \zeta_i) = \nabla_x J(x; \zeta_i)$. In this case, we only have access to an approximated loss function $\tilde{J}(x)$ and an estimated gradient

$$G(x; \xi_M) = \frac{1}{M} \sum_{i=1}^M G(x; \zeta_i) = \mathbb{E}_\zeta[G(x; \zeta)] + \xi_M = G(x) + \xi_M,$$

where the random variable ξ_M characterizes the random error in the gradient estimation. The relationship between ζ and ξ_M depends on the concrete form of $J(x; \zeta)$. Thus, (1.3) becomes

$$X_{n+1} = X_n - \eta_n \mathbb{E}_\zeta[G(X_n; \zeta)] + \eta_n \xi_M = X_n - \eta_n G(X_n) + \eta_n \xi_M,$$

where the noise term $\eta_n \xi_M$ is analogous to the $\sigma_n \psi_n$ term in (1.5), which we wish to control in our proposed algorithm. As discussed in [14], changing the batch size M is an effective way to control the power of the noise term given a fixed step size (see B1).

Next, we examine our proposed algorithm (2.1) with the control over the variance implicitly done through the adaptive batch size M_n . Consider

$$(5.4) \quad J_2(\mathbf{x}; \zeta) = J_1(\mathbf{x}) + \zeta^1 \sum_{i=1}^d \sin(10x_i) + \zeta^2 \sum_{i=1}^d \cos(10x_i), \quad \zeta = [\zeta^1, \zeta^2]^\top,$$

where J_1 is defined in (5.1), $d = 2$ and $\zeta^1, \zeta^2 \sim \mathcal{N}(0, 0.5)$. Again, we fix $a = b = 1$ in J_1 and then test cases where $c = 0.01$ and 0.05 . Note that $J_1(\mathbf{x}) = \mathbb{E}_\zeta[J_2(\mathbf{x}; \zeta)]$. We modify our proposed algorithm in

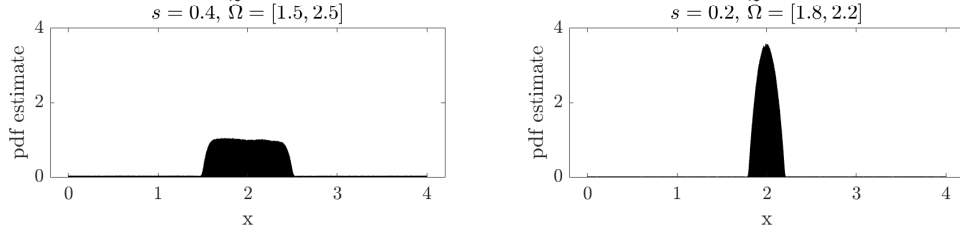


Fig. 8: Approximated density function of the invariant measure for (5.6) where the noise term follows (5.7). Left: $s = 0.4$, $\tilde{\Omega} = [1.5, 2.5]$; Right: $s = 0.2$, $\tilde{\Omega} = [1.8, 2.2]$.

the following way in terms of the batch size M_n :

$$(5.5) \quad X_{n+1} = \begin{cases} X_n - \frac{\eta_n}{M_n} \sum_{i=1}^{M_n} G(X_n; \zeta_i), & \frac{1}{M_n} \sum_{i=1}^{M_n} J_2(X_n; \zeta_i) < f_n, \\ \phi_n, & \frac{1}{M_n} \sum_{i=1}^{M_n} J_2(X_n; \zeta_i) \geq f_n, \end{cases}$$

where $M_n \in \mathbb{N}$ changes adaptively with n . Other notations follow earlier definitions in (2.1). To mimic the variance decay in the classical method (1.4), the batch size should follow $M_n = \mathcal{O}(\log n)$ [14]. For our proposed method (2.1), we may choose $M_n = \mathcal{O}(n^{2\alpha})$ where α is the constant in B3, but could be regarded as a tunable parameter in practical implementations. For the numerical test shown in Figure 7, we choose $M_n = \log(10n)$ for the classical method and $M_n = n$ for our proposed algorithm, with other parameters following the same setup as in Section 5.1.1.

In Figure 7, the proposed algorithm (5.5) yields an exponential convergence. As expected, the case $c = 0.05$ still converges faster than the case $c = 0.01$. On the other hand, despite the theoretical guarantee of global convergence, the classical $M_n = \mathcal{O}(\log n)$ decreases the variance very slowly and thus unable to give any visible convergence within 5×10^3 iterations. Comparing with Figure 5, the batch size-based setup yields slower convergence because not only the noise is no longer isotropic Gaussian as a result of its coupling with the gradient formulation, but also the loss function value now becomes an estimation $\tilde{J}(X_n) = \frac{1}{M_n} \sum_{i=1}^{M_n} J_2(X_n; \zeta_i)$. An important aspect of our proposed algorithm is to use the loss function value as an indicator to decide if $X_n \in \Omega_n$. In this example, the iterates are thus affected by the random error between $J(X_n)$ and $\tilde{J}(X_n)$, particularly so when close to the ground truth x^* . A slower decay rate of f_n is preferable for such situations.

5.2.2. Gradient-Free Optimization. We consider a modified algorithm compared to (1.5) where the gradient component is removed,

$$(5.6) \quad X_{n+1} = X_n + \sigma_n(f(X_n))\psi_n,$$

and enforce the periodic boundary condition for iterates that exit the domain $\Omega = [0, 4]$. Let $\sigma_n(f(x))$ be a piecewise-constant function where

$$(5.7) \quad \sigma_n(f(x)) = \begin{cases} s, & x \in \tilde{\Omega}, \\ 1/s, & \text{otherwise.} \end{cases}$$

for some $s > 0$. Here, $\tilde{\Omega}$ mimics the low-variance sublevel set Ω_n in earlier parts of the paper.

Starting with $X_0 = 1$, we compute $N = 2 \times 10^7$ iterations. We approximate the occupation measure

$$\mu_{X_0, T}(B) = \frac{1}{N} \sum_{n=1}^N \mathbb{1}_{X_n \in B},$$

where $B \subset \mathbb{R}^d$ is any Borel measurable set and $\mathbb{1}$ is the indicator function. Under mild conditions, $\mu_{X_0, T}$ converges to the physical invariant measure μ^* [23]. We estimate μ^* using N iterates; see Figure 8 for the estimated probability density functions based on two setups for the variance.

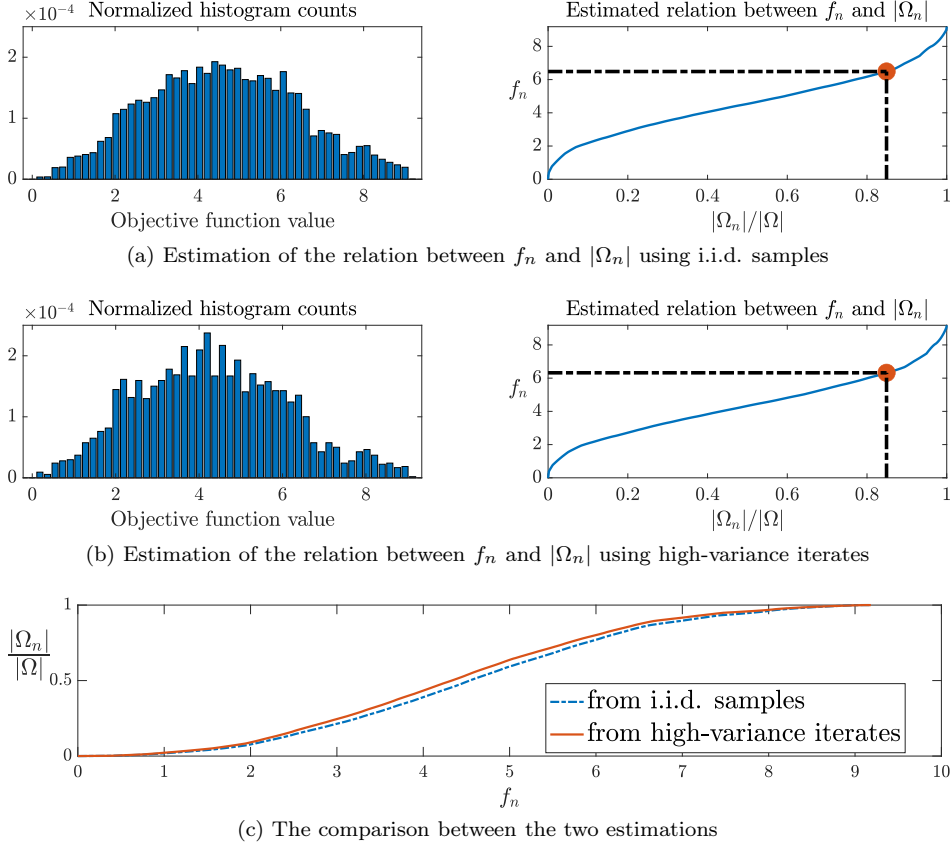


Fig. 9: (a) Estimation of the relation between f_n and $|\Omega_n|$ using i.i.d. samples; (b) Estimation of the relation between f_n and $|\Omega_n|$ using high-variance iterates; (c) A pointwise comparison between the two estimations of $|\Omega_n|$ as a monotonically increasing function of f_n .

When $s = 0.4$ and $\tilde{\Omega} = [1.5, 2.5]$, the stationary distribution concentrates on the small-variance region $\tilde{\Omega}$ while the density becomes more concentrated for the case of $s = 0.2$ and $\tilde{\Omega} = [1.8, 2.2]$, as seen in Figure 8. A comparison between the two plots shows the evident impact of the state-dependent stochasticity based on which the iterates are more likely to stay within the region of small variance.

In our proposed SGD algorithm (1.5) with the variance (1.6), in particular, algorithm (2.1), we utilize such property to align the small-variance region with the sublevel set of the objective function, which we aim to find the global minimizer. On the one hand, the iterate is more likely to stay within the sublevel set due to the small variance. On the other hand, as the iteration continues, the small-variance region shrinks as we decrease the cutoff value that decides the sublevel set. Finally, the iterate converges to the global minimizer in probability due to both aspects under properly chosen decay rates.

5.3. Estimating $\Omega^*(f)$. We illustrate the effectiveness of using high-variance samples to estimate $\Omega^*(f)$ through numerical examples. This corresponds to the earlier discussion in Section 4.2.1. Recall that $\Omega^* : \mathbb{R} \mapsto \mathbb{R}^+$ and $\Omega^*(f) = |\{x \in \Omega | f(x) \leq f\}|$. It is a function that maps the cutoff objective function value f to the volume of the f -sublevel set of the objective function $f(x)$. Again, we use J_1 in (5.1) as our objective function by setting $a = b = 1, c = 0.01, d = 2$. In Figure 9a, we draw $N = 1 \times 10^9$ i.i.d. samples $\{Y_i\}$ to produce a baseline result. The left-hand side plot is a histogram of $\{J_1(Y_i)\}$, which we could interpret as the empirical probability density function (pdf) for the random variable $J_1(x)$ where $x \sim \mathcal{U}([-20, 20]^2)$.

The right-hand side plot in [Figure 9a](#) is the corresponding estimated inverse cumulative distribution function (icdf). In our case, the icdf illustrates how the cutoff value f_n depends on $|\Omega_n|/|\Omega|$. Given the approximated icdf, one can use numerical interpolation to obtain a sequence of cutoff values $\{f_n\}$ such that the volume of the sublevel set $|\Omega_n|$ decreases following a desired rate.

Next, we use about 5.3×10^5 high-variance iterates $\{X_{n_k+1}\}$ ($\sigma_{n_k}(f(X_{n_k})) = \tilde{\sigma}_0 = 20$), generated as part of the SGD algorithm, to estimate the relation between f_n and $|\Omega_n|$. Note that we set $\tilde{\sigma}_0 = 20$ in [Equation \(5.2\)](#) for numerical illustration. We also remark that we do not need to store the iterates, but only their objective function values (real scalars). The similar two plots are shown in [Figure 9b](#). For $|\Omega_n| = 0.85|\Omega|$, the estimated f_n is 6.4855 using the i.i.d. samples, and 6.3233 using the high-variance iterates, as highlighted in both figures. A pointwise comparison of the estimated cumulative distribution function ($|\Omega_n|/|\Omega|$ as a function of f_n) based on the two approaches is presented in [Figure 9c](#).

6. Conclusion and Future Directions. In this paper, we have proposed AdaVar, a stochastic gradient algorithm [\(1.5\)](#) where the variance of the noise term is adaptive and state-dependent, with the goal of finding the global minimum of a nonconvex optimization problem. The algorithm is proven to have an algebraic rate of convergence in [Section 3](#) under quite general assumptions, and this is a substantial improvement over the current standard logarithmic rate. The main component of the proposed algorithm is to allow adaptivity of the variance so that it changes not only in time but also in the location of the iterates so that a stronger noise is imposed when the iterate yields a larger objective function value; see [\(1.6\)](#) for an example. If we know enough information about the objective function, the proposed algorithm costs the same as the classical method of simulated annealing. The techniques for accurately tuning parameters in the algorithms add very little to the overall computation cost. Several numerical examples presented in [Section 5](#) further demonstrate the efficiency of the algorithm.

There are quite a few future directions along the line of algorithms with state-dependent variance, which we here called AdaVar. Let us remark on the two briefly introduced and tested examples in [Subsection 5.2](#). First is the application to stochastic objective functions in [Subsection 5.2.1](#). As mentioned in [Section 1](#), the focus of this paper is on minimizing a given deterministic function and then adding a controlled stochastic component to achieve global convergence. A natural extension is the case where the stochastic component is directly linked to the objective function. This can either be because the objective function is intrinsically stochastic or, as is common in machine learning, a random sampling step is added to reduce the computational cost. There are two new challenges in this regime. One is the reduced control of the variance. In the machine learning case, natural tools include adjusting the batch size and controlling the adaptive step size, or the so-called learning rate. The other challenge is that only sampled values of the objective function are known. The sampling values can still be used, or different forms of aggregations or averaging could potentially be more representative.

Second, as illustrated in [Subsection 5.2.2](#), the steady-state distribution of a pure diffusion without the gradient term is also subject to the adaptivity of the noise variance as a function of the location. Therefore, it is possible to design a zeroth-order stochastic descent method for global optimization while embedding the information of the objective function into the noise term.

Another direction is to replace the use of an estimated Ω_n in determining the cutoff value f_n by using the escape rates from Ω_n to Ω_n^c in control-type algorithms. Finally, it is important to apply the algorithms in several realistic settings to adjust implementation details and to establish best practices.

Acknowledgment. We would like to thank the anonymous referees for their constructive comments that help us improve the quality of this paper. This work is partially supported by the National Science Foundation through grants DMS-1620396, DMS-1620473, DMS-1913129, and DMS-1913309. Y. Yang acknowledges supports from Dr. Max Rössler, the Walter Haefner Foundation and the ETH Zürich Foundation. This work was done in part while Y. Yang was visiting the Simons Institute for the Theory of Computing in Fall 2021.

- [1] S. BOYD AND L. VANDENBERGHE, *Convex optimization*, Cambridge university press, 2004.
- [2] R. E. CAFLISCH, *Monte Carlo and quasi-Monte Carlo methods*, Acta numerica, 7 (1998), pp. 1–49.
- [3] J. A. CARRILLO, S. JIN, L. LI, AND Y. ZHU, *A consensus-based global optimization method for high dimensional machine learning problems*, ESAIM: Control, Optimisation and Calculus of Variations, 27 (2021), p. S5.
- [4] Y. CHEN, Y. CHI, J. FAN, AND C. MA, *Gradient descent with random initialization: Fast global convergence for nonconvex phase retrieval*, Mathematical Programming, 176 (2019), pp. 5–37.
- [5] T.-S. CHIANG, C.-R. HWANG, AND S. J. SHEU, *Diffusion for global optimization in \mathbb{R}^n* , SIAM Journal on Control and Optimization, 25 (1987), pp. 737–753.
- [6] M. CHIANI, D. DARDARI, AND M. K. SIMON, *New exponential bounds and approximations for the computation of error probability in fading channels*, IEEE Transactions on Wireless Communications, 2 (2003), pp. 840–845.
- [7] R. M. CORLESS AND N. FILLION, *A graduate introduction to numerical methods*, AMC, 10 (2013), p. 12.
- [8] J. DONG AND X. T. TONG, *Replica exchange for non-convex optimization*, Journal of Machine Learning Research, 22 (2021), pp. 1–59.
- [9] W. E AND E. VANDEN-EIJNDEN, *Towards a theory of transition paths*, Journal of statistical physics, 123 (2006), pp. 503–523.
- [10] B. ENSING, A. LAIO, M. PARRINELLO, AND M. L. KLEIN, *A recipe for the computation of the free energy barrier and the lowest free energy path of concerted reactions*, The journal of physical chemistry B, 109 (2005), pp. 6676–6687.
- [11] X. GAO, Z. Q. XU, AND X. Y. ZHOU, *State-dependent temperature control for Langevin diffusions*, SIAM Journal on Control and Optimization, (2020), pp. 1–26.
- [12] S. B. GELFAND AND S. K. MITTER, *Recursive stochastic algorithms for global optimization in \mathbb{R}^d* , SIAM Journal on Control and Optimization, 29 (1991), pp. 999–1018.
- [13] S. GEMAN AND C.-R. HWANG, *Diffusions for global optimization*, SIAM Journal on Control and Optimization, 24 (1986), pp. 1031–1043.
- [14] W. HU, C. J. LI, L. LI, AND J.-G. LIU, *On the diffusion approximation of nonconvex stochastic gradient descent*, Annals of Mathematical Sciences and Applications, 4 (2019).
- [15] C.-R. HWANG AND S.-J. SHEU, *Large-time behavior of perturbed diffusion Markov processes with applications to the second eigenvalue problem for Fokker–Planck operators and simulated annealing*, Acta Applicandae Mathematica, 19 (1990), pp. 253–295.
- [16] S. KIRKPATRICK, C. D. GELATT, AND M. P. VECCHI, *Optimization by simulated annealing*, Science, 220 (1983), pp. 671–680.
- [17] H. J. KUSHNER, *Asymptotic global behavior for stochastic approximation and diffusions with slowly decreasing noise effects: global minimization via Monte Carlo*, SIAM Journal on Applied Mathematics, 47 (1987), pp. 169–185.
- [18] P. NATALINI AND B. PALUMBO, *Inequalities for the incomplete gamma function*, Math. Inequal. Appl, 3 (2000), pp. 69–77.
- [19] L. A. RASTRIGIN, *Systems of extremal control*, Nauka, (1974).
- [20] K. H. ROSEN, *Handbook of discrete and combinatorial mathematics*, CRC press, 2017.
- [21] C. TOTZECK, *Trends in consensus-based optimization*, arXiv preprint arXiv:2104.01383, (2021).
- [22] X.-S. YANG, *Nature-inspired optimization algorithms*, Academic Press, 2020.
- [23] L.-S. YOUNG, *What are SRB measures, and which dynamical systems have them?*, Journal of Statistical Physics, 108 (2002), pp. 733–754.
- [24] A. ZHIGLJAVSKY AND A. ZILINSKAS, *Stochastic global optimization*, vol. 9, Springer Science & Business Media, 2007.